Response to Reviewer 1 (Prof. Dr. Werner Eugster)

Dear Prof. Dr. Eugster,

Thank you for your detailed remarks and constructive comments which are all very helpful for improving the manuscript. We are glad that you find our work interesting and innovative. We are particularly grateful for the substantial work to understand all details, which will help us clarify the text and improve the presentation. As noted, our aim is to provide a detailed fully open-source description of the system that can contribute to more extensive data collection and to inspire technical improvements by the broader community. Our response to your specific review comments are given below.

2.1 Major issues

2.1 Referee comment (RC)1: The authors use three low-cost sensors, all from Figaro Inc.: the TGS2611-E00, the NGM2611-E13 (which uses the same TGS2611-E00), and the Panterra from Neodym (I assume), which in the version I used had a percursor version of the TGS2611 or so built in. I think the authors should more clearly specify (a) what sensor the Panterra uses (and provide the company names of all sensors), (b) clarify that these are (most likely) all the same sensors in different configurations (as it reads now the reader could be getting the impression that three different sensor types were tested, which is not the case)

2.1 Author response (AR)1: It is correct that all three sensors investigated are rather similar sensors from Figaro. The TGS2611-E00 and NGM2611-E13 differ in that the latter is attached to a small board with a potentiometer used for a crude factory calibration at 5000 ppm and with a 5-pin connector for easy plug-in to a system with a corresponding connector (cost efficient when handling many systems). The Panterra sensor is built around the Figaro TGS2610 sensor (order code PN-SM-GMT-A040A-W20A-05-R0- S0-E1-X0-I2-P0-L2-J1-Z0) from Panterra Neodym Technologies, Canada. This Panterra sensor, which was recommended after discussion with a Neodym technician, was the same as used in our study in Duc et al., 2013.

We selected sensors based on specifications and discussions with company representatives regarding several criteria, including methane specificity, a sensitivity that was potentially high enough for our applications, price and power consumption (more on this below), and believed that configuration and signal processing also can make a difference so testing different configurations was of interest to us. The sensor details were too spread out in our manuscript which we now realized was unclear.

2.1 Author changes in manuscript (ACM)1: The sensor details and motives behind the sensor selection will be provided in the same paragraph for all sensors together and early in the text. *Page 5 line 18.*

2.1 RC2: I am concerned about the low voltages that the TGS2611-E00 gives, ca. 18–35 mV according to Fig. 3. The TGS2600 that I use delivers 200-400 mV for ambient conditions, and when I look at the specifications it appears that the manufacturer considers the TGS2611-E00 to be useful in the range of 300–10,000 ppm CH_4 which is way above ambient range (the TGS2600 is shown with a sensitivity to CH_4 in the range 1–100 ppm CH_4 that's the reason we selected this one for near ambient measurements in Eugster & Kling, 2012). Now there are some other publications that show that the TGS2611-E00 is actually sensitive also to near ambient conditions, but I am not yet convinced that

this is the best choice for your application given the low CH_4 concentrations well below the range indicated on the technical specification sheet of the manufacturer. Some more critical discussion on the sensor selection would be required in my view.

2.1 AR2: This question highlights and revealed an error in the script for plotting the scale of Fig. 3A. The corrected Figure 3 is pasted below. The background level of the NGM2611-E13 sensor should be in the range of few hundred millivolts, in line with your expectations.

We first intended to try the TGS2600 sensor from your study with proven high sensitivity. When contacting Figaro, they recommended we try the TGS2611-E00 and NGM2611-E13 because we wanted a high specificity for CH_4 and because it have higher sensitivity than specified (the Product Information notes also indicate that the sensors are far from the detection limit at the low end of the tested range; 300 ppm). We decided to follow the Figaro technician suggestions as a start and simply kept working with them because they gave an adequate response for our applications (otherwise we would have tried the TGS2600). It should be noted that previous attempts to measure absolute ambient air levels is much more demanding in terms of sensitivity than our application, which is focusing on relative change, often with a doubling or more in levels over 1-2 hours. When assessing relative changes over time in a closed system it is also important to minimize interferences of other gases that may also change over time – further explaining our sensor choice as a trade-off between sensitivity and specificity.

2.1 ACM2: The error in the scale of Figure 3 have been corrected and clarifications on sensor details and motives behind the sensor selection will be made (see ACM1 above).

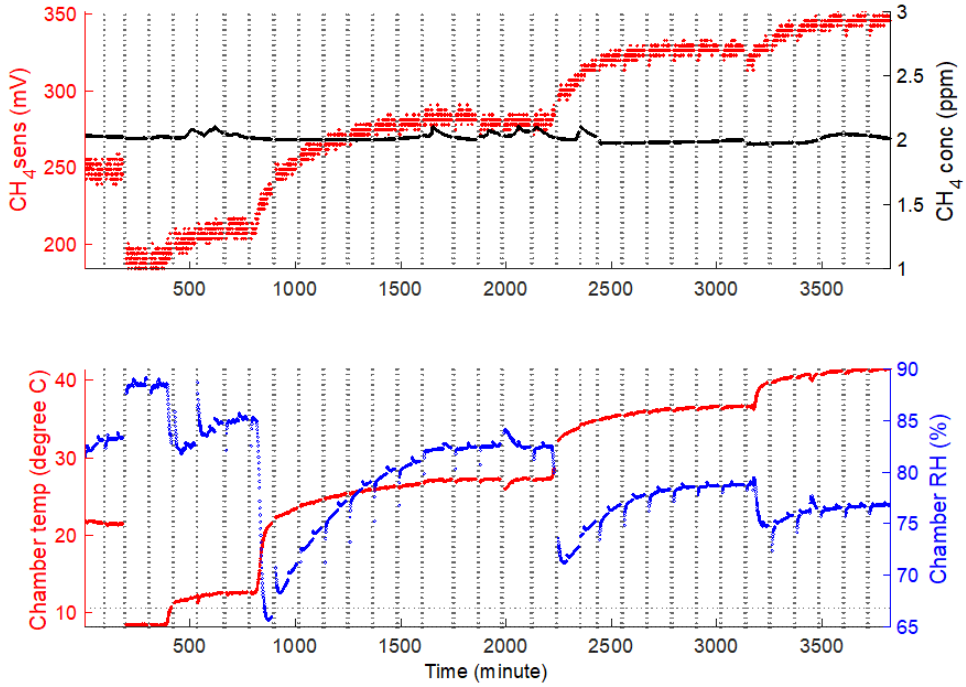

2.1 RC3: The authors only sample data every minute, which I find utterly coarse. They may have a reason for this, but in my own tests with the TGS2600 a one-minute measurement interval in combination with a 5-minute data rejection after chamber deployment (page 6, line 26; this information should actually have been given in the Methods section already, because this is an

essential flaw in the system in my view) I would have lost all the information relevant to chamber fluxes (see graph below and description of unpublished internal example graph from my experiments at Toolik Lake, Alaska, USA). Thus, the authors should more precisely describe their method and critically discuss such shortcomings to help others to do better.

2.1 AR3: One goal of our project was to develop an active wireless sensor network in which data from many flux chambers (called clients) are sent by Xbee radio transmitter modules and recorded on a small low-cost Raspberry Pi computer on the lakeshore. The sampling data rate, so far, is constrained to maintain the digimesh network working with minimum labor effort. In bad weather conditions, radio communication is easily broken, therefore it can take some minutes to re-establish the communication depending on the distance of the clients. During this offline period, the limited memory buffer of these data loggers does not allow us to sample very often. A second reason for the one-minute measurement internal is driven by coordinated logging and transmitting data from a CO_2/RH/Temp sensor having a 25 second measurement cycle – which also presently restricts the measurement frequency.

The rejection of data from the initial 5-minutes of measurements, is because the CH_4 sensor signal can be affected by temperature and relative humidity, and when focusing on relative change it is again important to minimize the influence of other confounding factors that may change over time. This rejection period is mainly to wait for temperature and relative humidity in the chamber to stabilize after chamber closure on the water surface to ensure that the CH_4 sensor response reflects CH_4 and not changing humidity and or temperature.

From your attached graph, it appears that the temperature and relative humidity in your chamber reach stable equilibrium quite quickly. In our case, we use the temperature and relative humidity measured from an integrated sensor onboard the CO_2 sensor which is measured every minute along with CO_2 concentration. Of course, an obvious data interpretation improvement would be to modify the length of the initial period during which data is not used to the actual time it takes to reach stable enough relative humidity and temperature, instead of having the static 5-minute period used here for simplicity.

In spite of our low measurement frequency, our results show that the system is still able to capture relative changes adequately. Of course, the situation is very different in applications aiming for accurate absolute levels in ambient air, and for such applications a high measurement frequency is of course more important to cancel out sensor noise in data processing than in our flux chamber application.

2.1 ACM3: The explanations and motivations provided above in AR3 will be clarified in the manuscript in a discussion paragraph devoted to measurement frequency. *Page 9 line 19, page 10 line 21.*

RC4: The ebullition (bubble) counter is quite interesting, but with a bubble volume of 3-4 mL required to actually leave a defensible signal, this does not yet seem to be an optimum choice. Here, a reference to and comparison with the (commercial) system of Andreas Mäck (doi:10.5194/bg-11-2925-2014) would be helpful. Since the Varadharajan et al. (2010) reference (pages 2,3,8, lines 30,22,21) is not listed in the References, I could not convince myself that this bubble counter system is really thoroughly tested and reliable. In the discussion you only say "For a long term solution, the recent study using optical sensors in an open path funnel (Delwiche and Hemond, 2017) 30 suggests an alternative and interesting design for ebullition studies, which could be combined with the present sensor approach to also quantify CH_4 content in the bubbles." – thus does this mean that you are

satisfied with the performance for short-term investigations? I am not really convinced and would appreciate a somewhat clearer statement what your recommendation is for studies that are shorter than a "long-term solution".

2.1 AR4: We apologize for the missing Varadharajan et al. (2010) reference and will correct this. We were not aware of the Meack et al 2014 paper and will integrate this to the manuscript.

Most previous bubble counter systems are based on bubble volume quantification by differential pressure sensors (e.g. Varadharajan et al. 2010; Maeck et al 2014) or optical sensors (Delwiche and Hemond, 2017). The detection limit of the differential pressure measurement, in our case corresponding to 3-4 ml gas, depends on the shape of the cylinder where the bubbles accumulate. Therefore, the longer and narrower a cylinder, the lower the detection limit. In turn, this leads to a trade-off, where the more sensitive systems become too tall for deployment in shallow waters, which often have proportionally higher ebullition rates. Our detection limit was chosen to allow deployment in shallow water. The shorter funnel of Delwiche and Hemond, 2017 (based on the optical sensor) combined with our system could solve the challenge we face deploying in shallow waters. We apologize that this statement was not clear in the manuscript.

2.1 ACM4: The response above including explanation of trade-offs and choices will be clarified in the revised manuscript. We will also more clearly relate to similar studies and have added proper references to Varadharajan et al 2010 and Maeck et al 2014. *Page 8 line 34*

2.1 RC5: Your regressions (I assume you use ordinary least-squares regressions) are not correct from a statistical viewpoint (Figs 4 and 5): you must reverse the dependent and the independent variable: you want to find out how to use the signal to compute the true concentration using your regressions, not the other way around (i.e. to predict the signal based on knowledge of the concentration – that's what your regressions show).

2.1 AR5: Figure 4 is to be seen as a calibration curve where the CH_4 concentrations are measured by reference instruments (GC-FID or an LGR greenhouse gas analyzer) and thereby represents the independent (x-axis) data. The CH_4 sensor response in the calibration case becomes the dependent signal. We agree that in a case when wanting to calculate concentrations from sensor signals, reversing the dependent and independent variables, would make more sense.

Figure 5 is just showing the sensor signal over time and simply provide temporal information of multiple variables (time on x-axis) and no regressions are made directly in this graph.

2.1 AMC5: A clarification that Figure 4 represents a calibration curve will be added.

2.1 RC6: I always use a fan in chambers, you don't. I understand that this corresponds to some static chambers that people use with syringe sampling, but in your case I am concerned that without a fan to mix the volume of the chamber the CO_2 (which is heavier than air) starts to accumulate above the water surface, and then a steep gradient creeps upwards where I expect your sensors; hence this linear increase in Fig. 5. Contrastingly, CH_4 which is lighter than air, quickly would accumulate under the top of the chamber, and hence probably the curvature although I would have expected that the CO_2 saturation should occur earlier than the CH_4 saturation in such a chamber. Please comment on this and justify why not to mix the air inside the chamber to ascertain representative concentration

measurements inside the flux chamber.

2.1 AR6: Our floating chamber is light-weight and freely moves up and down with the water. There is also some wind induced drifting around the separate anchored float. The sensors in the chamber are about 10 cm above water surface. We believe that the natural movement of chamber caused by winds and waves mixes the volume in the chamber.

We are aware of the vital need of air mixing in chambers holding vegetation, but for open water cases we see a risk that adding a fan will create an unknown bias from the added fan-induced turbulence and weight.

Some chambers designed differently have reported biased fluxes, while the chamber design used here without fans have repeatedly shown negligible bias compared to non-invasive techniques under variable conditions ranging from coastal water, small lakes and streams (Cole at al 2010; Gålfalk et al 2013; Lorke et al. 2015). Hence, we preferred to keep this tested chamber design.

2.1 ACM6: The choice of the chamber design and evidence in support of it will be clarified. *Page 1 line 37.*

2.1 RC7: According to the manufacturers information the sensor resistance decreases as the CH_4 concentration increases, thus in principle the voltage you measure should decrease not increase with increasing CH_4 – but your measurements in Fig. 4 show the exact opposite of what one would expect from the manufacturer information. Do you have an explanation for this? I must admit that on short timescales I see the same (see Figure inserted below), but on longer timescales I see what I would expect from the manufacturer's data sheet. Our procedure suggested by Eugster & Kling (2012) solve this issue with the calibration – after linearisation the use of a high and low calibration point simply reverses the sign if the response is of the kind that you show in Fig. 4. If you have an explanation why the TGS2611-E00 has increasing voltage with increasing CH_4 concentration then this would be a helpful insight for the reader. If you don't have an explanation, maybe you have an opinion?

2.1 AR7: From our understanding, the NGM2611-E00 and the TGS 2611 sensor in a circuit essentially operates as a voltage divider. A figure and associated text from the Product Information note of TGS 2611 (https://www.figaro.co.jp/en/product/docs/tgs2611_product_information_rev02.pdf) is provided below. The resistance of the CH_4 sensor is called Rs which has a resistance value that decreases as CH_4 concentration increases, load resistor R_L has constant value (about 5 kΩ). This circuit is fed by a constant circuit voltage V_C (5V), and the current equals to ratio of $5/(Rs+R_L)$. Hence, if Rs decreases, the current will increase. As a result, output voltage (V_{RL}) which equals to $R_L*5/(Rs+R_L)$ will increase. We have not studied the circuit details for other sensors so perhaps interpretations of the output voltage differ among sensors which may be the reason for this comment. We will double check our understanding and if it seems OK we will try to clarify this in the supplementary material.

Basic Measuring Circuit:

The sensor requires two voltage inputs: heater voltage (V_H) and circuit voltage (V_C). The heater voltage (V_H) is applied to the integrated heater in order to maintain the sensing element at a specific temperature which is optimal for sensing. Circuit voltage (V_C) is applied to allow measurement of voltage (V_{RL}) across a load resistor (R_L) which is connected in series with the sensor.

A common power supply circuit can be used for both V_C and V_H to fulfill the sensor's electrical requirements. The value of the load resistor (R_L) should be chosen to optimize the alarm threshold value, keeping power dissipation (P_S) of the semiconductor below a limit of 15mW. Power dissipation (P_S) will be highest when the value of Rs is equal to R_L on exposure to gas.

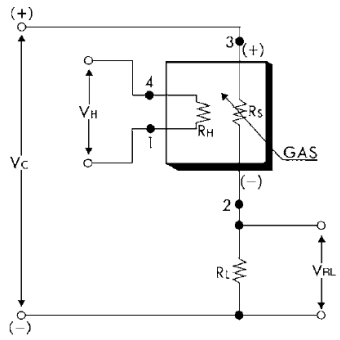

2.1 ACM7: The above explanation will be clarified in the supplementary material.

2.2 Minor Issues

2.2 RC1: p2/33: "The eddy covariance (EC) technique is increasingly used for long-term monitoring, but it is expensive in terms of equipment and is still being evaluated for aquatic environments." – what do you mean with this statement? I don't consider this to be correct, the method is in use beyond evaluation. Please provide some references and reword the second part. For example, we have authored a couple papers and also written a chapter in the book Eddy Covariance: A Practical Guide to Measurement and Data Analysis (chapter on lakes: doi:10.1007/978-94-007-2351-1_15). Thus, the method is established (at least better than your chambers, to be more direct) – but I agree that it is costly and I agree that such low-cost sensors are important.

2.2 AR1: We did not intend to unfairly describe EC measurements. Given the discussions on issues such as lateral fluxes (land/sea breeze effects), wind shadow zones around forested lake shores, other irregularities in wind patterns over lakes, challenges interpreting footprint locations and shape for small lakes, and other discussions on suitable equipment (e.g. open or closed path gas analyzers), we simply had the impression that method evaluation and development was still ongoing. Because the referee comment clearly signals we were wrong we will remove this statement.

2.2 ACM1: We will reword the sentence to: "The eddy covariance (EC) technique is increasingly used for long-term monitoring of terrestrial and lake-dominated landscapes, but it is expensive in terms of equipment." *Page 2 line 35.*

2.2 RC2: p2/45: " The CH4 sensor tested here is a Taguchi Gas Sensor (TGS) (Figaro Engineering Inc., Osaka, Japan). It is a high sensitivity CH_4 gas sensor. . . ": I completely disagree, it is a low-sensitivity sensor which (in the version you use) only has a manufacturer specified lower measurement range of 300 ppm CH_4! I already realize that our more cautious wordings about the TGS2600 (which has a higher sensitivity than the TGS2611-E00) is ignored by some others, which can lead to frustration. Be clear that this is experimental work trying to squeeze the tiny bit of information out of a sensor that is not made for ambient concentrations – but I agree that it has some value for such measurements.

2.2 AR1: We meant that the sensor is more sensitive than several other CH_4 sensors in the same prize class, but we agree with the reviewer and now see that the statement can be interpreted in misleading ways.

2.2 ACM2: We will remove this statement (See also AR2.1, AR2)

2.2 RC3. You never specified which pressure sensor you used, thus it is unclear to me why you did not use an I2C sensor, there plenty of those on the market. What is the special advantage of your pressure sensor that requires an AD620 amplifier to be useful? This remains obscure to the reader.

2.2 AR3 This manuscript describes work that is a follow up from a previous study on an automatic system to measure greenhouse gases from aquatic environments (Duc et al., 2013). In our previous electronic circuit, we used an AD620 amplifier for the pressure sensor (26PCDFA6G, Honeywell, Sensing and Control, Canada) to measure atmospheric pressure. After reading the work of Varadharajan et al. (2010), we adapted our system by simply changing one external resistor to get the proper gain factor to use with our pressure sensor (26PCAFA6D).

2.2 ACM3: We will add the sensor information and clarify our reasons for choosing this sensor to the manuscript. *Page 3 line 23*.

2.2 RC4: Eq. 1 should use SI units or at least the same units of the same physical quantity and not include obscure conversion factors. Thus, you must decide whether your time variables should be in hours or in seconds (the primary SI unit) or minutes, please no mixtures.

2.2 AR4: The flux time unit was in hours representing a relevant time unit given the accumulation time of the chamber. As this study focuses on evaluating the sensor response to the change in mixing ratio of CH_4 and CO_2 gases in the chamber in which the sensor signal is recorded every minute, we have decided to present $\Delta C/\Delta t$ (ppmv min^{-1}) to avoid applying a conversion factor.

2.2 ACM4: The above explanation will be provided in the manuscript. *Page 5 line 13*.

2.2 RC5, p5/25: check your instrument information, most likely this was an LGR FGGA (not a DLT-100, which as I remember is a CH_4-only instrument) that measures CH_4 and CO_2.

2.2 AR5: The reviewer is correct - instrument we used is an early benchtop version of the FGGA analyzer that have the capacity to measure CH_4, CO_2 and H_2O. It has DLT-100 printed on the cover leading to this confusion.

2.2 ACM5: We will edit the manuscript to include "a FGGA with capacity to measure CH_4, CO_2 and H_2O." *Page 5 line 36*.

2.2 RC6, p6/8: you did not specify what your "baseline noise" actually is. Is it the square root of the variance or the noise baseline derived from an Allan variance plot, or anything else? Some more details in the Methods section would be really helpful.

2.2 AR6: Our baseline noise is square root of the variance.

2.2 ACM6: We will add this clarification to the manuscript. *Page 6 line 14*.

2.2 RC7 p6/13: "The pressure in the trap was affected by air temperature, especially the diel temperature cycle." – this sounds like an error, pressure is a physical entity that is independent of temperature, thus this must be wrong. What I can imagine is that you mean that your pressure sensor signal (but not the pressure itself) depended on air temperature. Please correct.

2.2 AR7: We did mean to refer to the pressure sensor signal.

2.2 ACM7: We will correct this in our manuscript to read "The pressure sensor signal measured in the trap was affected….". *Page 6 line 19*.

2.2 RC8 p8/39: "However, since the sensor is not calibrated for very high concentrations, we could not determine the flux rate observed during these events." – I completely disagree, at least for CH_4 (you do not really reveal any necessary details on the CO_2 measurements . . .): the TGS2611-E00 has a specified measurement range from 300 to 10,000 ppm according to the manufacturer. Although the sensors come uncalibrated (at any concentration, not only at high ones), this wording is not correct. Maybe you wanted to say that you did not calibrate the sensor at higher concentrations, but the sensor per se is always uncalibrated from this manufacturer.

2.2AR8: Correct and thanks. We did not calibrate the sensor at higher concentrations.

2.2 ACM8: We will edit this statement in the manuscript to read "However, since we did not calibrate the sensor for high concentrations, we could not determine the flux rate….". *Page 9 line 11*.

2.2 RC9 p9/14: "The Panterra CH_4 sensor signal has been compensated for the temperature effect, but is probably not applicable for temperatures lower than 15°C." – please give the details of the sensor used in the Panterra (it is a TGS if you use the same model that I used years ago and threw away because it was unreliable); as it is, this statement is pure speculation and should either be removed or substantiated with some arguments.

2.2AR9: The Panterra sensor product features identifies that it has active temperature compensation (http://neodymsystems.com/download/Panterra-MOS-ALL_Brief_101.pdf). We did try calibrating at temperatures lower than 15°C but still the sensor deviated in its response from other TGS sensors. We did not do further testing to investigate this response because it seemed more efficient to focus on the other sensors.

2.2 ACM9: We will remove this sentence from the manuscript as we did not investigate this further.

2.3 Feedback on Supplementary Information
2.3 RC1: in PowerControlBoard.zip remove the deleted file
~$Copy of Bomexample(1).xlsx

2.3 ACM1: We will remove this unused file.

2.3 RC2: in BOM_PWCv8c_digikey.xlsx remove unused "Sheet1"

2.3 ACM2: We will remove "Sheet1".

2.4 Technical issues
- homogenise your variable names in text and figures (d0CH_4sens, d0_CH_4sens, d0_CH_4sensor; d0CH_4conc, d0_CH_4conc, d0_CH_4concentration, d0CH_4concentration)
- decide whether you want to use upper case or lower case letters in figure panels
- use a space between axis title and parentheses around units
- use a degree sign where a degree sign is required (not 0)
- define all your variables that appear in text and figures
- spell out abbreviations upon first occurrence (e.g. AFC on p2/39)
- use some more adequate natural intervals in time axes (e.g. Fig. 5: start at midnight

00:00 and then use 3-hour intervals not some 2:24 hour intervals)
- make figure captions standalone so that the figure is understandable without reading the entire text; also define all symbols and line types (maybe a legend could help)
- do not use the term “plot” for lines or symbols in a panel of Fig. 1
- remove the erroneous and confusing superfluous ticks at the right border of panels (b) and (c) in Fig. 1
- Fig. 2: conventionally panels are labeled from left to right, then top to bottom (which would group a,b and c,d in your caption); explain what each line type indicates and what the symbols with vertical stems indicate.
- Fig. 3: add the 0 label at the beginning of the time axis; I would call this "Elapsed time" and put minute into plural
- add subscript in CH_4 in Fig. 3 caption and everywhere else where this was forgotten.

2.4 ACM1: We will update the manuscript to include all the above changes.

References:

Duc, N. T., Silverstein, S., Lundmark, L., Reyier, H., Crill, P., and Bastviken, D.: Automated Flux Chamber for Investigating Gas Flux at Water–Air Interfaces, Environ. Sci. Technol., 47, 968-975, 10.1021/es303848x, 2013.

Cole, J.J., Bade, D.L., Bastviken, D., Pace, M.L. and Van de Bogert, M. (2010) Multiple approaches to estimating air-water gas exchange in small lakes. Limnology and Oceanography-Methods 8, 285-293.

Gålfalk, M., Bastviken, D., Fredriksson, S. and Arneborg, L. (2013) Determination of the piston velocity for water-air interfaces using flux chambers, acoustic Doppler velocimetry, and IR imaging of the water surface. Journal of Geophysical Research: Biogeosciences 118, 770-782.

Lorke, A., Bodmer, P., Noss, C., Alshboul, Z., Koschorreck, M., Somlai-Haase, C., Bastviken, D., Flury, S., McGinnis, D.F., Maeck, A., Muller, D. and Premke, K. (2015) Technical note: drifting versus anchored flux chambers for measuring greenhouse gas emissions from running waters. Biogeosciences 12, 7013-7024.

Maeck, A., Hofmann, H., and Lorke, A.: Pumping methane out of aquatic sediments – ebullition forcing mechanisms in an impounded river, Biogeosciences, 11, 2925-2938, https://doi.org/10.5194/bg-11-2925-2014, 2014.

Varadharajan, C., Hermosillo, R., and Hemond, H. F.: A low-cost automated trap to measure bubbling gas fluxes, Limnology and Oceanography: Methods, 8, 363-375, 2010.

Response to Reviewer 2 (Dr. Maciej Bartosiewicz)
Dear Dr. Bartosiewicz,

Many thanks for your valuable comments and detailed remarks on our manuscript and your suggestions to improve the system. We very much appreciate your review efforts that will be very helpful in improving our manuscript.

As noted earlier, we aim for providing a detailed, fully open-source description of the system that can contribute to more extensive data collection and to inspire technical improvements by the broader community. Our response to your specific review comments are given below.

1.0 RC 1: This is an excellent and timely description of low-costs system allowing to monitor fluxes of CO2 and CH4 in aqautic setting with relatively high precision. I believe that this article/techincal note is suitable for publication but further care must be taken to improve the presentation. The text reads well mostly but a few places the flow should be improved. I think that even a Technical Notes will get more attention if properly streamlined. Also, and most importantly, I strongly suggest that a visual representation of the sampling system is included in the main body of the paper. I found some illustrations in the SI but a compact and clear technical scheme of the described system should be available in the main ms. After these rather minor issues are resolved I recommend this draft for publication.

1.0 AR1: Given that this type of manuscript is expected to be short we decided to move the visual representation to the supplemental information (SI) section.

1.0 ACM1: We will discuss with the editor if we can add a more substantial visual representation of the sampling system to the main body of the paper. *Moved Figure S5 from SI to become Figure 1 in manuscript.*

1.0 RC2 Page1 Line 35: You state that " the flux chamber method which can trap both diffusive and ebullitive (bubble) fluxes, has been demonstrated to not bias gas fluxes at the air water interface" There is a number of publications (see Vachon et al. 2010 for example) providing evidence that chambers themselves can affect turbulence (and thus the flux) at the water- air interface. I also support using chambers as reference direct method for flux estimation but you should, at least, acknowledge that there is a potential effect on turbulence from the static chamber.

1.0 AR2: Clear turbulence effects have been noted for some chambers designs/approaches, such as chambers attached to a stationary and heavy objects (e.g. ADV instrument in the mentioned reference), while the chamber design used here, with light weight, limited intrusion of chamber walls into the water, and chamber mooring to enable the chamber to following wave or water motion as much as possible, has repeatedly shown negligible bias compared to non-invasive techniques under variable conditions ranging from coastal water, small lakes and streams (Cole at al 2010; Gålfalk et al 2013; Lorke et al. 2015).

1.0 ACM2: As we have stated in Response to Reviewer 1 comments *2.1 ACM6:* The choice of the chamber design and evidence in support of it will be clarified. In this clarification we will show awareness of the possible turbulence effects as suggested here. *Page 1 line 37.*

1.0 RC3 (line 1-5, page 2): You later state that (line 1-5, page 2) "these methods are inexpensive in terms of equipment and work well to quantify gas emission in a confined area but they are labor intensive and have low temporal resolution" This is correct if the gas inside of the chamber is somehow homogenized. I understand that this is, in fact, tedious and adds another layer of complexity

but I found it better to have a pump connected on the top of the chamber that would mix the gas inside. Otherwise, during longer deployments, CO_2 can accumulate inside your chamber and may bias the flux estimates.

1.0 AR3: In our statement "*these methods are inexpensive in terms of equipment and work well to quantify gas emission in a confined area but they are labor intensive and have low temporal resolution* ", we were referring to the entire sampling process which in most sampling setups on a lake requires traveling (often rowing) out to deploy and then returning some time later to sample and returning samples to the laboratory for analyses. We agree also that adding the manual mixing of the headspace also adds time.

1.0 ACM3: We will correct the sentence in the manuscript to read "*Both these methods are inexpensive in terms of equipment and work well to quantify gas emission in a confined area however they are labor intensive due to repeated visits for both deployment and sample collection and therefore often have low temporal resolution." Page 2 line 4.*

1.0 RC4 (line 30 page 2): Using eddy covariance is well established in lakes – please reword your statement; aside from being costly and logistically complex to install, eddy covariance datasets often require labour intensive re-processing. . . but it is certainly well established.

1.0 AR4: As in our response to reviewer 1 comments 2.2 AR 1, we did not intend to unfairly describe EC measurements. Given the discussions on issues such as lateral fluxes (land/sea breeze effects), wind shadow zones around forested lake shores, other irregularities in wind patterns over lakes, challenges interpreting footprint locations and shape for small lakes, and other discussions on suitable equipment (e.g. open or closed path), we simply had the impression that method evaluation and development was still ongoing. Because the referee comment clearly signals we were wrong we will remove this statement.

1.0 ACM4: We will reword the sentence to: "The eddy covariance (EC) technique is increasingly used for long-term monitoring of terrestrial and lake-dominated landscapes, but it is expensive in terms of equipment." *Page 2 line 35.*

1.0 RC5: Specify what is the sensor in your Panthera (Neodym?), it sounds to me that these three configurations use the same methane sensor. . . "TGS2611-E00 sensor is equipped with a filter to reduce the influence of interference" what filter???? Please specify as this may be important for future use.

1.0 AR5: The manufacturer does not provide information about the filter in the product description only that it is meant to "eliminate the influence of interference gases such as alcohol, resulting in highly selective response to methane gas".

1.0 ACM5: We will modify the sentence to include this information from the manufacturer: "The TGS2611-E00 sensor is equipped with a filter to eliminate the influence of interference gases such as alcohol, resulting in a selective response to CH_4.". and we will add the manufacturer's product website (http://www.figarosensor.com/product/entry/tgs2611-e00.html) as a reference.

1.0 RC6: There seems to be a problem with your bubble counter as limiting your measurements to bubbles are larger than 3-4 ml may bias total flux estimates, would it make sense to use a pre-trapping system for small bubbles?? I do not know how would/if this can be integrated but imagine a system

that when CH_4 bubble is detected but not quantified because of its low volume then it is directed toward another trap where cumulative volume of such small bubbles can be assessed?

1.0 AR6: We appreciate the suggestion for modification to pre-trap small bubbles. We decided on this design of an "accumulation trap" so that all the bubbles will be trapped, but the limitation in technology and the variable conditions of deployment outdoors does not allow us to resolve very small bubbles.

1.0 ACM6: We will clarify that ours system accumulates all bubbles and perform the measurements when the bubble volume is large enough. Hence the limited resolution of small bubbles does not mean that the small bubbles are missed but more that the pressure sensor measurements do not resolve individual small bubbles but instead measure the average volume of many bubbles. *Page 6 line 23*.

1.0 RC7: You state that: "If bubbles entered the trap and were large enough to activate the venting mechanism during a non-logging period, it was missed in the logged data file" How often did this happen during your experiments and what was the size of bubbles activating venting.

1.0 AR7: The upper threshold of the bubble trap is a technical feature of the trap design however we have not observed this during any of our tests. In this study the accumulated bubble volume of 28 ml will activate the venting, and we did not experience any bubble events larger than this threshold, but we think it is important to report this setting and the need to consider it to potential users.

1.0 ACM7: We will add a statement to clarify this in the manuscript. *Page 6 line 30*.

References:

Cole, J.J., Bade, D.L., Bastviken, D., Pace, M.L. and Van de Bogert, M. (2010) Multiple approaches to estimating air-water gas exchange in small lakes. Limnology and Oceanography-Methods 8, 285-293.

Gålfalk, M., Bastviken, D., Fredriksson, S. and Arneborg, L. (2013) Determination of the piston velocity for water-air interfaces using flux chambers, acoustic Doppler velocimetry, and IR imaging of the water surface. Journal of Geophysical Research: Biogeosciences 118, 770-782.

Lorke, A., Bodmer, P., Noss, C., Alshboul, Z., Koschorreck, M., Somlai-Haase, C., Bastviken, D., Flury, S., McGinnis, D.F., Maeck, A., Muller, D. and Premke, K. (2015) Technical note: drifting versus anchored flux chambers for measuring greenhouse gas emissions from running waters. Biogeosciences 12, 7013-7024.

Greenhouse gas flux studies: An automated online system for gas emission measurements in aquatic environments

Nguyen Thanh Duc[1,4], Samuel Silverstein[2], Martin Wik[3], Patrick Crill[3], David Bastviken[4], Ruth K. Varner[1]

[1]Institute for the Study of Earth, Oceans and Space and Department of Earth Sciences, University of New Hampshire, Durham, 03824, USA
[2] Department of Physics, Stockholm University, 106 91, Sweden
[3] Department of Geological Sciences, Stockholm University, 106 91, Sweden
[4]Department of Thematic Studies - Environmental Change, Linköping University, 581 83, Sweden

Correspondence to: Nguyen Thanh Duc (thanh.duc.nguyen@liu.se)

Abstract. Aquatic ecosystems are major sources of greenhouse gases (GHG). Robust measurements of natural GHG emissions are vital for evaluating regional to global carbon budgets and for assessing climate feedbacks on natural emissions to improve climate models. Diffusive and ebullitive (bubble) transport are two major pathways of gas release from surface waters. To capture the high temporal variability of these fluxes in a well-defined footprint, we designed and built an inexpensive device that includes an easily mobile diffusive flux chamber and a bubble counter, all in one. In addition to automatically collecting gas samples for subsequent various analyses in the laboratory, this device also utilized a low-cost carbon dioxide (CO_2) sensor (SenseAir, Sweden) and methane (CH_4) sensor (Figaro, Japan) to measure GHG fluxes. Each of the devices were equipped with an XBee module to enable a local radio communication (DigiMesh network) for time synchronization, and data readout at a server-controller station on the lakeshore. Software of this server-controller was operated on a low-cost computer (Raspberry Pi) which has a 3G connection for remote control and monitor functions from anywhere in the world. This study shows the potential of a low-cost automatic sensor network system to study GHG fluxes on lakes in remote locations.

1 Introduction

Despite the fact that lakes and impoundments only cover around 3.7% of the continental area (Downing et al., 2006;Verpoorter et al., 2014), their contribution to global carbon dioxide (CO_2) and greenhouse gas (GHG) budgets are substantial (Tranvik et al., 2009;Bastviken et al., 2011). Lake emissions are not only large, but previous studies also highlight large uncertainties in overall emission estimates. For example, a recent synthesis of CH_4 emissions from northern lakes and ponds reveals that these aquatic environments contribute 16.5 Tg CH_4 yr^{-1}, equivalent to more than 65% of inverse model calculation of all natural CH_4 sources in the region where CH_4 fluxes were believed to be largely emitted from wetlands (Wik et al., 2016b). In addition, the climate sensitivity of natural emissions of GHGs is not well understood, but metadata analyses showed that CH_4 emissions and the ratio of CH_4 to CO_2 emissions increase markedly with the increasing temperature (Yvon-Durocher et al., 2014;Marotta et al., 2014). Previous field studies of GHG emissions are still limited in their spatial and temporal resolution, which potentially result in poorly resolved measurements and biased estimates (Wik et al., 2016a). For this reason, there is a need for new and improved approaches to study the emission of CH_4 and CO_2 from open, fresh water ecosystems at both higher temporal and spatial resolutions.

Using conventional techniques with well-defined footprints, emitted gases can be trapped in air-filled flux chambers (FC) or submerged water-filled funnels (Chanton and Whiting, 1995). When properly designed with a light weight chamber that has limited intrusion into the water surface, a mooring to enable the chamber to follow wave and water motion, the flux chamber method, which can trap both diffusive and ebullitive (bubble) fluxes, has been repeatedly shown to have negligible bias in gas flux measurement at the air-water interface relative to SF_6 assessments (Cole et al., 2010) or other independent non-invasive methods (Gålfalk et al., 2013;Lorke et al., 2015). A submerged funnel moored to allow movement around a specified area can be deployed to specifically trap gas bubbles released from the sediment surface (Wik et al., 2013). For both flux chambers and submerged funnels, the trapped gas is commonly collected manually with syringes after a specific time interval, and analyzed in the laboratory. Both methods are inexpensive in terms of equipment and work well to quantify gas emission in a defined relatively small area. However, they are labor intensive due to the need for repeated visits for both deployment and sample collection and therefore often result in low temporal resolution of emission measurements. During short term measurements, there is also a high probability of missing potentially rare and episodic ebullition events entirely. In contrast, during long term chamber or funnel deployments, CH_4

dissolution and or oxidation in the water that is in contact with the trapped gas could result in an underestimation of flux. Most previous measurements reported in the literature were based on infrequent measurements within short time frames (0.5 to 24 hrs) and likely did not capture ebullition in a representative way thereby resulting in underestimation (Wik et al., 2016a). As a result, there is a high uncertainty in extrapolations and modeling of CH_4 and CO_2 emissions over time from open water ecosystems (Smith, 1985;Walter et al., 2001;Bastviken et al., 2004;Meng et al., 2012). High frequency measurements over long periods with broad spatial coverage of studied areas could reduce this uncertainty and result in more representative gas emission estimates. Regarding the floating chamber approach, there are automated methods in which the trapped gases in the chamber can be sampled with a system of pipes and large pumps connected to a gas analyzer (Goodrich et al., 2011;Goulden and Crill, 1997). This can better address the temporal variability, but the gas analyzer equipment is typically expensive. The chambers also need to be relatively close to the gas analyzer so this method can be limited in spatial coverage.

Carbon dioxide flux measurements require a short time period for chamber deployment due to rapid equilibration. There are commercially available high precision CO_2 sensors available (e.g: Li-Cor, Vaisala-CO_2) (Johnson et al., 2010;Anderson et al., 1999) which can be connected to chambers for CO_2 analysis. However, their cost makes it difficult to afford many simultaneous measurements across a study area. Recently, Bastviken *et al*. (2015) proposed the use a low-cost CO_2 sensor and developed applications for pCO_2 and CO_2 flux measurement in outdoor environments.

High frequency measurements of the timing of ebullitive events have been made using techniques based on video/photo or hydro acoustic methods (Ostrovsky et al., 2008;Tassin and Nikitopoulos, 1995). Acoustic methods have a high potential for solving the spatial heterogeneity of gas emission, but this technique can have a high cost for equipment and there remains some uncertainty in quantifying gas emissions (Ostrovsky et al., 2008;DelSontro et al., 2015). In addition, these techniques may work well in ecosystems with frequent ebullition, but sonar scanning can be time and power consuming over extended periods in ecosystems where ebullition is less frequent. In such systems, there is a need for inexpensive and power-efficient equipment for long term, continuous monitoring of ebullition. Varadharajan et. al (2010) developed a low-cost automated trap to measure ebullition flux using an inverted funnel connected to a pressure sensor whose signal was recorded by a commercial data logger. This type of commercial data logger and funnel still requires manual maintenance and gas release which also means a high potential for missing ebullition events when the trap is full of gas. The eddy covariance (EC) technique is increasingly used for long-term monitoring of terrestrial and lake-dominated landscapes, but it is expensive in terms of equipment (Vesala et al., 2012;Deemer et al., 2016). In addition, EC measurements were not designed to account for any small-scale spatial variability from different types of areas that lies within the footprint of the measurement.

To increase the quality and quantity of observations of aquatic GHG emission, we developed a low-cost, simple, robust and portable device with a well-defined footprint for investigating gas flux at the water-air interface. This is a follow up from our previous open-tech published work focused on measuring CH_4 using an automated flux chamber (AFC) (Duc et al. 2013), now substantially improved by including sensors to reduce the need of laborious manual sampling and analyses, a wireless on-line readout-control device that has the capability to simultaneously measure ebullitive fluxes by an automatic bubble counter (ABC) and diffusive CH_4 and CO_2 fluxes by an automated floating chamber. Taking advantage of small, low cost CH_4 and CO_2 sensors, we have modified our AFC, which is composed of a flux chamber connected to an automated control box (Duc et al., 2012), to measure CH_4 and CO_2 flux from aquatic environments. The CH_4 sensors tested here were Taguchi-type semi-conductor Gas Sensors sold by Figaro Engineering Inc., Osaka, Japan or Panthera Neodym Technologies, Canada (sensors described below).. Eugster and Kling (2012) showed successfully that a similar sensor (TSGS2600) has potential to measure CH_4 at ambient air concentrations. The sensors have a high sensitivity to relative humidity and temperature, but these responses can be corrected for to yield corrected CH_4 signals (see below). The CO_2 sensor used here (CO_2 Engine ELG K33, from SenseAir, Sweden) is a low-power module that measures CO_2, temperature and relative humidity. Therefore, this CO_2 sensor can provide temperature and humidity data to correct the CH_4 sensor response. The sensor-equipped AFCs were combined with submerged funnels for automated detection of bubbles (the ABC). Here, we suggest a solution to automatically collect or release the trapped gas, and restart the bubble trap by using a pump and valve system, which are controlled by an inexpensive microcontroller-based data logger, based on the feedback of the pressure signal.

2. Methods

In this section, we describe the technical details of our new device (a combined AFC and ABC) that simultaneously measures CH_4 ebullition and diffusive CH_4 and CO_2 emissions. This device operates and

communicates (to receive working parameters and send data) within a digimesh network using a Xbee transmitter module (XBP24-AUI-001J, Digi International, USA). The system consists of a floating control box that houses the electronics, a floating chamber and a submerged funnel (Figure 1). The control box is a watertight case which stores a power source (either a 12V 7Ah lead-acid battery or a 12V 55Ah lithium ion battery (Power Pack LS 55, vuphongsolar.com, Vietnam), diaphragm pumps, electronic valves, a pressure sensor and the electronic controller boards inside, and had a solar panel mounted on the top of the box. The control box connects to either the chamber or the funnel or both of them. Compared with the previous version in Duc et al. (2013), the electronic controller boards, including the power control board and the data logger board, have been redesigned to include an open 5Vdc supply for a CH_4 sensor, an open I2C connection for a CO_2 sensor, and an open UART2 connection for XBEE radio communication.

2.1 Ebullition counter

The ABC was based on an inverted funnel design similar to (Wik et al., 2013) adopting the measurement principle of Varadharajan et Al. (2010). From the funnel stem, a 30-cm PVC pipe (10 mm I.D.) was attached to accumulate bubbles. The maximum trapped bubble volume for this system is ~ 28 mL. The other end of the PVC pipe was attached to an inverted 10 mL syringe whose tip was connected to a differential pressure sensor (26PCAFA6D, Honeywell, Sensing and Control, Canada; this sensor was chosen for being similar to Varadharajan et al. (2010) and being compatible with the electronics in our system) via a polyurethane tube (3.175 mm inner diameter, Clippard URT1-0805; Figure 1). The pressure sensor was power by regulated 10Vdc; its signal was amplified 495-fold by an AD620 chip (Analogue Devices; USA). Gas accumulating in the pipe pushes down the water level relative to the water level outside the pipe, and this water level difference generates a pressure that is proportional to the gas volume in the pipe. The ebullition rate (mL/min) is determined from the change in the differential pressure inside the pipe over time; therefore, it is important to make the trap gas tight.

The ABC can be programed to simulate the deployment cycle of a manual trap including capturing bubbles and releasing of gases when the trap is full. To enable autonomous operation for long deployment periods, not only the pressure sensor but also a pump and a 2-way valve were connected to the bubble trap via the polyurethane tube and two T-connectors (Figure S1). The pump and valve were powered by 12Vdc.

The microcontroller-based datalogger board continuously reads the amplified pressure sensor signal, and a step-wise pressure increase from gas accumulation indicates an ebullition event that is recorded with date and time stamps. The bubble measuring cycle of the ABC in the field includes initiation, measurement and ventilation stages. In the initiation state, the pump injects a small amount of air (about 5 mL) into the sampler to push any condensation water droplets out of the tube and to have a starting pressure equivalent to the sensor detection limit. During the measurement state, bubbles are trapped in the funnel and the pressure signal is continuously monitored by the datalogger. When the pressure signal increases to a threshold level indicating that the bubbles have filled up the PVC pipe, the headspace of trapped bubbles can be either vented away or measured in a connected CH_4 and CO_2 sensor box. The controller activates a ventilation cycle in which the pump purges the trap, and then the valve opens for ventilation. The valve closes again when the pressure signal drops down to the initial detection limit level. This also prevents water from entering the tube which could cause moisture blockage interfering with sensor response. The ventilation stage cycles three times until the headspace is replaced by air. This measuring cycle (Figure S1) makes the ABC fully automated and operational over long periods - week to months or perhaps years given adequate power supply.

The pressure data can be recorded either to an SD card on the data logger or by wireless transfer to an onshore computer for subsequent transfer to a cloud server (See Section 3.3 Wireless network in Supplementary material). The data file is then processed (Matlab, etc) to extract the ebullition events from baseline noise based on the stepwise increase of the pressure signal. When the ABC was deployed in the field, the baseline noise increased. Even if the pressure sensor is pre-calibrated and has a temperature compensated range from 0 to 50°C, the weather conditions, including temperature, wind and waves, will physically affect (shrink or expand) the bubble in the trap. Therefore, the noise removal is a critical procedure in data processing to extract the bubble events.

The regular electric noise, drift, and wind/wave effects on the pressure sensor generate high frequency low level signals. A bubble, on the other hand, will generate an abrupt jump that raises the level of pressure signal (Figure 1). In general, this leads to periods with constant average pressure separated by a finite number of abrupt signal jumps to new pressure levels due to bubbling. This reflects a piecewise constant signal (Little and Jones, 2011). The noise in the signal needs to be removed to identify the timing and volume of ebullitive events. The classical noise removal solvers, such as smoothing, or filtering over a moving window, have several limitations when a signal can abruptly change, and these abrupt changes of pressure signals are what need to be allocated and preserved. From our field measurement data, the noise, which generally is symmetric and tailed caused by

temperature changes (Figure 1), can be removed by the jump penalization method (Little and Jones, 2011). This jump penalization solver was chosen based on the observed results from 10 different noise removal solvers that were included in a "piecewise constant toolbox" (http://www.maxlittle.net/software/). This toolbox implements algorithms for noise removal from 1D piecewise constant signals, such as total variation and robust total variation denoising, bilateral filtering, K-means, mean shift and soft versions of the same, jump penalization, and iterated medians (Little and Jones, 2011). After the noise was removed, the denoised data is composed of flat regions at different pressure levels and the boundary of those regions. The pressure levels are proportional to the volume of bubbles in the trap and the locations of the jumps are the time when bubbles enter the trap. These events were detected by applying point-wise (1st order) differentiation calculations on the denoised data. The positive differentiates, with peak heights greater than three times the standard deviation of the baselines, were identified as ebullition events. A report data file including date, time of the ebullition event and sizes of bubble were exported as a text file.

2.2 Measuring CH_4 and CO_2 flux in the AFC.

The AFC system presented in Duc et al. (2013), was improved by equipping the floating chamber with previously described low cost CH_4 and CO_2 sensors. To protect these sensors in high humidity environment, their electronics boards were coated by polyurethane resin (arathane 5750 or Ultifil 3000-010, details are in Section 1.1 Sensor coating in Supplementary material). To prevent water splashing, the sensors were placed in a protected plastic box with holes for air through-flow mounted in the chamber. A detailed design is described in Bastviken *et al*. (2015), however in this study the condensation protection sheet was not used. A rubber tube (230x65 mm Inner Tube Straight Valve Stem, Part # 952932367600, esska.se) was attached to the chamber to automatically open/close the chamber for ventilation or accumulation phase by inflating and deflating the tube, respectively.

The CH_4 sensor was configured as shown in Eugster and Kling (2012). It is powered with 5Vdc and its analog signals are recorded via the analog input of the datalogger board (Duc et al., 2013). The CO_2 sensor data, including CO_2 concentration, relative humidity and temperature, were transferred to the datalogger via an I2C connection. The CO_2 sensor is powered with 10Vdc. The CO_2 sensors which were used in this study were prepared as described in Bastviken et al. (2015). In the recorded data file, in addition to the time stamp and sensor data, there is a chamber open/close marker. This helps to identify the accumulation and ventilation phases of the chamber. These data are post-processed with a script (written in Matlab, MathWorks, USA) to determine the fluxes during the chamber accumulation period.

Methane flux is determined based on the change of filtered CH_4 sensor signals over an accumulation period. The filter is set to select data period in which the variation of RH and temperature in the chamber are small enough to not affect CH_4 sensor signals. The diffusive flux is estimated from the best linear increase of CH_4 sensor signals without ebullition event. Additional details are presented in the CH_4 sensor calibration section. The CO_2 sensor was tested previously for use in flux chambers to determine CO_2 emission (Bastviken et al., 2015). The slope of the CO_2 concentration linearly changing in the time range, which has R^2 higher than 0.98, is extracted as the rate of CO_2 emission per time. In our field study, the chamber is closed for 100 minutes and open about 20 minutes for ventilation, and data from the sensors was output every 1 minute. The GHG flux is calculated using the following equation.

$$F = \frac{\Delta C}{\Delta t}\frac{PV}{RT}\frac{60 * 10^{-6}}{A} \qquad \text{Eq. 1}$$

where F is flux (e.g. mol m^{-2} h^{-1}), $\Delta C/\Delta t$ is change in GHG mixing ratio over time in the FC headspace (ppmv min^{-1}), P is atmospheric pressure (atm), V is the FC volume (6300 mL), R is the gas constant (82.0562 mL atm K^{-1} mol^{-1}), T is the temperature (K), A is surface area of the FC (0.069 m^2), 60 is a conversion factor from min^{-1} to h^{-1} and 10^{-6} is a conversion factor from ppmv to fractional mixing ratio measured in the gas. The flux time unit is in hours representing a relevant time unit given the accumulation time of the chamber. As this study focuses on evaluating the sensor response to the change in mixing ratio of CH_4 and CO_2 gases in the chamber in which the sensor signal is recorded every minute, the $\Delta C/\Delta t$ (ppmv min^{-1}) is used to demonstrate the response of CH_4 and CO_2 sensors.

2.3 CH_4 sensor test and calibration

We tested three commercial based TGS sensors for CH_4 including: TGS2611-E00, NGM 2611-E13, and a Panterra CH_4 sensor. The TGS2611-E00 sensor is equipped with a filter to reduce the influence of interference gases such as ethanol, resulting in a more selective response to CH_4 (Figaro, 2013). The NGM 2611-E13 is a pre-calibrated module for natural gas alarms, which is also based on the TGS2611-E00 sensor. This module is prebuilt as a gas detector circuit with a standard pin connector. The Panterra CH_4 sensor (PN-SM-GMT-A040A-W20A-05-R0- S0-E1-X0-I2-P0-L2-J1-Z0, Panterra Neodym Technologies, Canada) which is based on a TGS2610 sensor, has been pre-calibrated by the manufacturer. We chose the specific sensor versions in dialogue

with sensor company representatives, based on several criteria, including CH_4 specificity, a sensitivity that was potentially high enough for our applications, price and power consumption.

The responses of the CH_4 sensor to concentration, temperature and relative humidity (RH) in the chamber were studied, as well as the effect of hydrogen sulfide (H_2S), which is a potential inference gas released from some sediments. On a water tank in the laboratory, the AFC was set to close on water surface for 100 minutes and open 20 minutes for ventilation. Water temperature was regulated at different temperatures from 10 to 35°C. In temperature sensitivity experiment, the starting CH_4 concentration was atmospheric background levels (about 2 ppm), at which temperature were varied. In the calibration experiments, at different temperature levels, about 10 mL of CH_4 1000 ppm was injected into the 7 L chamber every 5 minutes until the AFC activates the ventilation process. About 5 minutes after the injection, a 10-mL gas sample from the chamber was withdrawn and injected into a gas chromatograph equipped with a flame ionization detector (GC-FID) to measure CH_4 concentration to be compared with sensor retrieved values. This test was repeated and, in later, the headspace gas in the chamber was circulated through a spectrometric gas analyzer (an FGGA with capacity to measure CH_4, CO_2 and H_2O; Los Gatos Research Inc.) for continuous CH_4 and CO_2 concentration measurements.

The H_2S interference experiment was carried out by injecting different volumes (from 2 to 637 mL) of standard gas H_2S 100 ppm (Duotec AS, Denmark) into the test AFC. The chamber headspace gas was circulated through a Biogas analyzer (Geotechnical Instrument, England) for measuring molecular oxygen (O_2) and H_2S. These results were analyzed using the JMP Pro software and Matlab to determine noise levels, quantitative flux determination limits, and a calibration equation.

2.4 Field deployment and monitoring

The field tests were performed on lakes at Stordalen Mire located in Abisko, Sweden (Wik et al., 2013). The floating control box was tied to a buoy, which was anchored to the lake bottom. The funnel and the chamber were attached to the control box with distance of 0.5 and 1 m, respectively. The funnel and chamber were able to freely move around the anchor point in an area of about 2 m radius.

3. Results

3.1 Bubble counter calibration experiment

Calibrating the bubble counter revealed that the pressure sensor cannot detect the first 5 mL gas in the trap due to the low accumulation pressure (Figure S2). Therefore, to reach the detection limit of the pressure sensor, the automatic bubble counter is started (prime pressurized) by pumping approximately 5 mL of air into the trap. This offset the ABC response in every measurement cycle. At pressures above this low-end threshold, the pressure sensor response showed a linear response to the volume of the gas captured in the trap. The upper threshold for a volume change that the trap can detect depends on the length of the extension PVC pipe. The longer extension pipe, the wider linear range of the bubble counter. Therefore, the ABC was programmed to end a bubble trap period by venting trapped gas before the extension pipe is completely filled with gas.

In stable conditions in the laboratory, the square root baseline signal (baseline noise) of the bubble trap at all pressure levels in the linear calibration curve is approximately 0.013 V. The detection limit calculated from three times the noise (0.039 V) is equivalent to about 0.8 mL. This means that our sensitivity is good enough to detect a bubble volume of 1ml – corresponding to a bubble size that has high occurrence probability in lake systems (Wik et al., 2013). In post data processing, any stepwise increase signal that is smaller than 0.04 V was therfore ignored. Field deployment data and the processed signal from a pressure sensor used to extract the bubble events are shown in Figure 1. The pressure sensor signal measured in the trap was affected by air temperature, especially the diel temperature cycle. If there is no bubble in the trap, the pressure signals fluctuate around a certain median value (Figure 2a). Small bubbles that enter the trap, do not create a strong increasing stepwise signal that was easily distinguished relative to the background noise. However, small bubbles still raised the pressure signal median which can be detected by the jump penalization solver (Figure 2b). Even if individual small bubbles are not resolved, their combined contribution to the trapped gas will be detected as increasing average differential pressure. The larger bubbles (around 3 - 4 mL) made clear stepwise increases in the pressure signal beyond the background noise and the jump penalization solver was able to extract the median of this stepwise pressure level. Larger bubbles therefore were determined with better resolution. Two cycles of bubble accumulation over a long-term field deployment from two tested devices shows that a wide variability of bubble sizes can enter the trap, from small bubble sizes (1 - 2 mL) who's signal is buried in the noise, to a large bubble (> 6 mL) that creates a large pressure signal compared to the background (Figure 2). If bubbles entered the trap and were large enough to activate the venting mechanism during a non-logging period (in the present system this

would require a total bubble volume > 28 ml), it was missed in the logged data file. However, no single bubble events larger than this threshold were experienced in the field tests so far.

3.2 AFC CH_4 sensor calibration experiment

The response of the CH_4 sensor, when the chamber closed on water surface, to changing temperature, RH, and CH_4 concentration (around 2ppmv), is shown in Figure 4. In the first few minutes after chamber closure, the temperature and RH changed quickly in the chamber, causing a drift in the CH_4 sensor signal, but once temperature and RH stabilizes, the sensor responded in a predictable way to changes in CH_4 concentration inside the chamber. After temperature and RH stabilization occurred in the chamber, we determined the detection limit of our instrument for CH_4 fluxes based on the noise of the CH_4 sensor. In these blank experiments, the RH was always in the range of 60 - 90%, which is within the sensor RH operating range. The operation of the CH_4 sensor includes heating it to a high temperature to detect combustible gases, therefore, the temperature inside the sensor box is always higher than the water temperature. The temperature sensor of the ELG CO_2 sensor measured the changing of temperature inside the sensor box over the water temperature. The noise over a whole accumulation period (100 minutes) was about 2.44 ± 1.21 mV. A minimum accumulation rate limit is calculated as five times the noise or about 12.2 mV. Therefore, we calculated the CH_4 concentration increase that generated a CH_4 sensor signal of 12.2 mV to be equivalent to 5.25 ppm and used this to calculate a minimum detectable CH_4 flux. In an accumulation period, the accumulation rate detection limit of this sensor embedded in the chamber is 5.25 ppm per 100 minutes (0.0525 ppm per minute).

At all temperatures (10, 20, 25 and 30°C), the three CH_4 sensor signals were well correlated to CH_4 concentration but these correlation lines had different intercepts depending on water temperature (Figure S3 a-c). The absolute concentrations measured by the sensors were affected by temperature and RH and were not suitable for use. To study CH_4 flux, we instead used the relative change of CH_4 concentration over time from five minutes after chamber closure to avoid the periods with the largest changes in temperature and RH. Accordingly, the differential CH_4 sensor signal ($d0\_CH_4sens$), which is the difference between the current measurement and the initial measurement point 5 minutes after the chamber closed on water surface, was used instead of the raw output signal from the sensor. Indeed, the differential CH_4 sensor signal was less sensitive to temperature and had a linear response ($r^2 = 0.98$; $p < 0.001$) across the studied temperatures (Figure 5). In this test, the variability in the temperature and RH were in ranges of 2°C and 5%, respectively, while CH_4 concentration increased from atmospheric or about 2 ppm to 25 ppm. The standard least square fit model was applied on $d0\_CH_4sens$ as a model response and the changing CH_4 concentration, temperature and RH as model effects. The result showed that the variability of temperature ($p = 0.038$) and RH ($p = 0.867$), have less influence on the CH_4 sensor response compare to the CH_4 concentration (p_value < 0.001). This reveals that these CH_4 sensors can be used to measure CH_4 flux when the temperature and RH conditions are stable in the chamber.

The effect of temperature and RH can be corrected for in the response of the sensor using an algorithm developed by Eugster and Kling (2012), but this was not applied in our study because we were not able to simulate the natural variations of outdoor temperature and RH conditions on our control experiment. Therefore, periods with stable temperature and RH were used and the calibration curve for the TGS2611-E00 CH_4 sensor in our application was the average linear response of $d0\_CH_4sens$ versus the changing of CH_4 concentration ($d0\_CH_4conc$) without temperature and RH correction (Figure 5)

$$d0\_CH_4sens = 1.256 \times d0\_CH_4conc + 5.871 \qquad \text{Eq. 2}$$

where $d0\_CH_4sens$ is the voltage change of the CH_4 sensor in mV, and $d0\_CH_4conc$ is in ppmv. Comparing with this sensor, calibration results showed that the pre-calibrated Figaro NGM2611-E13 module has about the same response to the change in CH_4 concentration at all temperatures. The NGM2611-E13 had a regression equation as following:

$$d0\_CH_4sens = 1.116 \times d0\_CH_4conc + 1.771 \qquad \text{Eq. 3}$$

The Panterra CH_4 sensor showed a different response at different temperatures (Figure 4). Its calibration lines had different response at 10 and 15°C, and its $d0\_CH_4sens$ has negative response when $d0\_CH_4conc$ is higher than 15 ppm at 20 and 30°C.

In the H_2S interference test, the injected volume of H_2S standard increased from 2 to 637 mL. The Biogas analyzer did not detect any H_2S even when the estimated H_2S concentration in the chamber was 9 ppm. This level is close to the detection limit of the instrument, and given the minimum analytical uncertainty of ± 10 ppm, it is likely that H_2S was present in high enough amounts to affect the CH_4 sensors. During the H_2S addition, the

CH_4 sensor signal increased to more than 5 times of baseline noise; therefore, H_2S was considered to affect the sensor response, in agreement with sensor producer tests.

3.3 CH_4 and CO_2 flux with the AFC

The pilot field deployment of the AFC embedded CH_4 and CO_2 sensors showed that the system was effective for measuring the variation of CH_4 and CO_2 concentration in the chamber over time (Figure 6 a-c). The automatic mechanism developed to close the chamber for flux measurements and open the chamber for ventilation periods/phases helped to reduce condensation and allowed for a linear response of the CO_2 sensor (Figure 6b). This is an improvement over past work and allows for the sensor to be deployed in the field for long time periods. There was a situation when the chamber was closed on water surface for a whole night due to a low-battery. As a result, the saturated RH in the chamber became higher than 100% and caused condensation and malfunction in the sensor until drying (discussed in Bastviken et al. 2015). After two ventilation cycles, the CO_2 sensor dried and the baseline decreased to the normal linear response range. The CO_2 sensor responses were not affected by temperature and RH in our experiment. Therefore, CO_2 flux is determined from the slope of the best linear response data in an accumulation period.

During measurement periods, right after ventilation, CO_2 concentrations in the chamber are supposed to be equal to the atmospheric CO_2 concentration above the lake surface. These initial CO_2 concentrations varied within a range of 516 - 1179 ppmv with higher mixing ratios during nighttime. Because the chamber ventilation time was early in the development adjusted to allow complete ventilation of the chamber headspace, the elevated starting concentrations may reflect actual concentrations if stable atmospheric conditions resulted in a near-ground buildup of CO_2 released from the lake and the surrounding mire ecosystem.

The field deployments revealed that there were many periods in which temperature and RH conditions of the chamber were stable enough (Figure 6a) for the Figaro CH_4 sensors to adequately measure the changing of CH_4 mixing ratio in the chamber. In cases where temperature and RH varied a lot, the data processing script determined periods of data where the variation of temperature and RH was less than 2°C and 5%, respectively, defining periods for which CH_4 sensor data could be reliably evaluated. If ebullitive CH_4 entered the chamber headspace, there was a clear positive change in the sensor signal output. This was easily identified as a stepwise increase of the CH_4 sensor signal over a very short time. This signal identified the type of ebullitive flux that could be measured over that chamber closure period. For diffusive CH_4 flux measurements, the d0_CH_4sens data, with a sensor response of less than 30 mV (within linear calibration range) and without a stepwise jump, were scanned for a data range with best linear adjusted R square. For diffusive flux estimation, the $\Delta C/\Delta t$ (ppmv min^{-1}) in Eq. (1) is calculated using the last d0_CH_4sens point in this linear range, in which d0_CH_4sens is converted to d0_CH_4conc (ppmv) follow Eq. (2) and its coordinate in time since the chamber closed is calculated the measurement period (minute). The manually collected gas samples in the field and the CH_4 mixing ratio change over time (ppmv/time) in the chamber headspace determined from the sensor response showed a strong linear relationship with a deviation of less than 15% (Figure 7). The ebullitive CH_4, which detected by the CH_4 sensor in the AFC, was not concentration quantified in this study focusing on the relative changes of the methane sensor in the low range, because CH_4 sensor response to ebullition events was usually out of the linear calibration range.

4. Discussion

4.1 Automated ebullition measurements using pressure sensors

Deploying pressure sensors to determine the timing of ebullition events and to measure the bubble volumes has been thoroughly tested by Varadharajan et. al. 2010. Our bubble trap introduces a way to automatically reset the system after being full of gas, that allows for long-term deployment with minimum maintenance effort. This design idea is similar to the automatic bubble traps in Maeck et. al. (2014). Further, via the jump penalization noise removal method, bubble events can be detected despite the noise caused by changes in air temperature affecting the bubble volumes and therefore the differential pressure . It is important that the ABC is gas tight. This is not a simple requirement; especially because the trap is built from plastic materials meant to be easily disconnected for portability and is exposed to the outdoor environment. After a long deployment time, leaks were occasionally observed at the assemble joint of the pressure sensor. So far, if a trap leak occurs, the pressure is lower than the priming pressure threshold, which was set to trigger a warning indication to the host server controller on the lakeshore. It can be fixed by applying glue on the leak site. The detection limit of the differential pressure measurement, in our case corresponding to 1-2 ml gas, depends on the shape of the cylinder where the bubbles accumulate (Maeck et al., 2014;Varadharajan et al., 2010). Therefore, the longer and narrower a cylinder, the lower the detection limit. This leads to a trade-off, where the more sensitive systems become too

tall for deployment in shallow waters, which often have proportionally higher ebullition rates (Wik et al, 2013). Our detection limit was chosen to allow deployment in shallow water with a trap height of about 0.5 m. The recent study using optical sensors in an open path funnel (Delwiche and Hemond, 2017), that makes a shorter trap, suggests an alternative and interesting design for ebullition studies, which could be combined with the present sensor approach to also quantify CH_4 content in the bubbles.

4.2 Automatic measurement of CH_4 and CO_2 during chamber fluxes

In our application, the low cost CH_4 and CO_2 sensors can be used to measure changing CH_4 and CO_2 concentrations. It is a direct approach to measure CH_4 and CO_2 flux from a defined-footprint area on the time scale of minutes-hours, extending over long-time periods given a suitable power supply. The chamber captures both ebullition and diffusion fluxes. Ebullition events are marked by abrupt changes in the response of the CH_4 sensor and therefore can be identified readily. The diffusive flux is identified by the gradual change in CH_4 and CO_2 concentration over time. We did observe ebullition events in the chamber during deployment periods, in support of the previous indications that ebullition typically accounts for a large share of the open water flux (Figure 6c). However, since we did not calibrate the sensor for high concentrations, we could not determine the flux rate observed during these events. This remains a challenge for future work.

To study diffusive fluxes, it is important to measure the change of gas concentrations during a short period of time right after the chamber closes. This requires a gas sensor that can measure at near ambient gas concentrations. The CH_4 injection experiment showed that both of the Figaro CH_4 sensors have sensitivity at low ppm mixing ratios and yield a linear response from ambient at about 2 ppm up to 25 ppm. The TGS2611-E00 and NGM2611-E13 have small differences in their response (slope) in the linear range, however, their responses to experimental conditions are overall very similar because they use the same sensor base. In outdoor field conditions, after closing on the water surface, it takes some time for temperature and RH in the chamber to stabilize. The rejection of data from the initial 5-minutes of measurements is important to select an initial CH_4 sensor data point when the temperature and RH has become more stable to minimize the influence of these confounding factors on the relative change of CH_4 sensor signal. An obvious data interpretation improvement would need to modify the length of the initial period during which data is not used to the actual time it takes to reach stable enough relative humidity and temperature, instead of having the static 5-minute period used here for simplicity.

It is possible that the sensors can be used outside the range reported here by developing other calibration curves. In any case, we recommend to adjusting the AFC accumulation time to the effective range of the sensor. Alternatively, flux calculation can be based on data within the linear range only in the post-processing of the data. Calibration for the Figaro CH_4 sensor is recommended for each individual sensor. The response slopes of different sensors could deviate up to 12%. For practical reasons, if flux estimation with tolerance ±20% error is accepted (Wik et al., 2016a), one general calibration line can be obtained from a calibration of at least five CH_4 sensors for statistical representativeness. In our study, the calibration line was obtained from the calibration experiment of eight sensors. Due to the effect of temperature and RH, the calibration curve should be based on calibration data at different water temperatures that span anticipated field conditions. Compared to Duc et al., 2012 which used the Panterra CH_4 sensor, the Figaro CH_4 sensor gave more reliable and robust flux measurement result under field conditions.

The H_2S interference test revealed that H_2S, a corrosive gas which can be released from anoxic sediments in sulfur rich systems, may interfere with sensor response. Therefore, extra care and thorough data validation is suggested when applying the sensors in sulfur rich environments. In addition, this CH_4 sensor response is based on reaction between O_2 in air and reductant (flammable) gases; therefore, any change in concentrations of either O_2 or reductant gases could interfere the signal of the sensor. This CH_4 sensor can combust a small amount CH_4 gas (about 0.0041 ppmv per minute), which needs to be considered when the CH_4 flux is low (near the detection limit 0.0525 ppmv per minute of the sensor in our application) and chamber accumulation time is very long.

One limitation of the CH_4 sensor is its power consumption. While the CO_2 sensor can be activated once per minute (or at other desired time intervals), the CH_4 sensor needs to be heated at all times. In our case, these systems were deployed at high latitudes in the summer and the battery was recharged by a 13W solar panel. If the weather was cloudy for four to five days in a row, the battery voltage fell below 10.5 V. At this point, the system automatically turns off until the battery is recharged. In 2017, the replacement lithium ion battery (12V 55Ah; Power Pack LS 55) helped to keep the system working continuously during longer time periods and reduced the weight of control box.

Over our deployment time, there were several chambers that were either submerged or turned over. The chambers were submerged because the rubber inner tube degraded due to UV exposure over a long period of

time, generally about two sampling seasons. This problem was solved by covering the inner tube with aluminum foil or by changing to the gas delivery flow scheme shown in Figure S9 ("no sink AFC"). With this new flow design, the air in the floating control box was pumped into the rubber inner tube until the inner tube is full. When the pressure inside the rubber inner tube is more than 1 psi, the check valve opens, the excess air is blown into the chamber to refresh its headspace. Compare with previous gas flow design, in which the air is withdrawn from the chamber, this new gas flow scheme will prevent under pressure built up in the chamber during the ventilation process; hence even in a situation where the chamber cannot open due to failure of the rubber inner tube the chamber will not sink. With this configuration, the sample array presented in Duc et al (2013) cannot be used. The strong correlation between grab samples and the sensors (Figure 7) allow us however to capture the high temporal fluxes and skip the labor-intensive process of analyzing grab samples. Manual grab samples should however be taken periodically as a cross check of the sensor response. The other problem of chamber flipping was caused by wind suddenly change its direction during chamber ventilation process. To prevent this flipping, the opening side of the chamber was attached with two floating anchors (called anti-flipping anchor) (Figure S10). With this improvement, there have been no chamber flip during tests with maximum wind speeds of about 7 m/s.

4.3 Challenges when networking measurement systems remotely

One goal of our project was to develop an active wireless sensor network in which a small low-cost Raspberry Pi computer on the lakeshore communicates with many flux chambers and bubble traps (called clients) by Xbee radio transmitter modules 2.4 GHz. The communication is to synchronize real date time, working parameters, to check client status and to receive data from clients. The sampling sensor data rate, so far, is constrained to maintain the digimesh network working with minimum labor effort. Under harsh weather conditions (rain and hard wind), radio communication is easily broken, and then it can take some minutes to re-establish depending on the distance and number of the clients. During this offline period, the limited memory buffer of the client data logger did not allow a very high measurement frequency. As a result of this limitation, one-minute data sampling interval was used to provide stability for long-term deployment. In spite of our low measurement frequency, the results show that the system is still able to capture relative changes in CH_4 concentration adequately. This situation is different from applications that aim for accurate absolute concentrations in ambient air, and for such applications a high measurement frequency is more important to cancel out sensor noise in data processing than in our flux chamber application. In our AFC system, higher frequency data, can be recorded in a local 2 GB SD memory on the datalogger of each trap if desired.

In our study, the traps were on the lake surface which was usually lower than ground level and surrounded by tree and plants. Over the study season, the growth of vegetation on the lakeshore can potentially block the line-of-sight between the host controller and the traps on the lake, which can hamper radio communication. To guarantee radio communication, at least one client (i.e. chamber system) was placed on a strategic location which had a clear line of sight to the host controller. Within the digimesh network, XBee modules can form a self-configuring, self-healing wireless peer-to-peer network with other data loggers in radio range. Therefore, the host controller doesn't necessarily need to have direct line-of-sight communication with all of the traps on the lake surface. If some of the traps are out of the controller's direct range, they should be automatically passing their messages through closer clients. Therefore, it is important to keep a robust network topology.

Occasional errors within this network still occur, probably due to high humidity environment around the clients and variable weather conditions, temperature and humidity (Luomala and Hakala, 2015). This could cause failure in transfer of some initial data packets in the data file or break the communication with clients. Hence, software for this system was developed to address these errors. For example, all the data packets were encoded, so the missing data can be easily identified in the post data processing and the host controller keeps searching to reestablish communication with "lost" clients. Details of wireless communication protocol and host-controller design are presented in the Supplementary material.

5. Conclusions

Resolving diffusive and ebullitive GHG fluxes at the air-water interface in a well-defined footprint area is needed so that we can accurately represent open water bodies likes lakes and streams in global CH_4 and CO_2 budgets. With the benefit of low-cost technology, we have modified simple flux chambers and bubble traps to function automatically with wireless remote monitoring and control via an internet browser. These traps are equipped with not only the sensors to monitor the fluxes in high temporal resolution but also the electro-mechanical hardware to do complex actions in the field such as venting traps and collecting gas samples (if needed). This is our first attempt to integrate several low-cost technologies to make a device to measure GHG

emissions from lakes with the data updated online in real time. This device, as an open source technology for non-profit academy study, can hopefully contribute to studies of GHG emission from aquatic environments in remote and logistically difficult areas.

Code availability

Data Availability

Supplement link

(from Copernicus)

Author contributions.

NTD: hardware, software designed the AFC-ABC system, conducted the study, developed Matlab script and processed data and co-wrote the manuscript; SS: hardware, core-software designed the wireless datalogger, webserver and contributed to the manuscript; MW conducted the study and contributed to the manuscript; PC, DB, RKV gave advice through all stages of the study, contributed funding, and co-wrote the manuscript. All authors discussed the results and commented on the manuscript.

Competing interests.

The authors declare that they have no conflict of interest.

Acknowledgements

This research was supported through a postdoctoral fellowship funded by the University of New Hampshire. The field deployments 2014 and 2015 were supported through two US National Science (NSF) grants to Ruth Varner: MacroSystems Biology (EF# 1241937) and the Northern Ecosystems Research for Undergraduates program (NSF REU site EAR#1063037); and by funding from the Swedish Research Council VR to David Bastviken and Patrick Crill (Grant no. 2012-00048). Work time for data analysis and manuscript preparation was also financed by VR grant no. 2016-04829, European Research Council (ERC) grant no. 725546, FORMAS grant no. 2018-01794 and VINNOVA grant no. 2015-03529.

References

Anderson, D. E., Striegl, R. G., Stannard, D. I., Michmerhuizen, C. M., McConnaughey, T. A., and LaBaugh, J. W.: Estimating lake-atmosphere CO2 exchange, Limnol. Oceanogr., 44, 988-1001, 10.4319/lo.1999.44.4.0988, 1999.

Bastviken, D., Cole, J., Pace, M., and Tranvik, L.: Methane emissions from lakes: Dependence of lake characteristics, two regional assessments, and a global estimate, Global Biogeochemical Cycles 18, GB4009, doi:4010.1029/2004GB002238., 10.1029/2004GB002238, 2004, 2004.

Bastviken, D., Tranvik, L. J., Downing, J. A., Crill, P. M., and Enrich-Prast, A.: Freshwater Methane Emissions Offset the Continental Carbon Sink, Science, 331, 50, 10.1126/science.1196808, 2011.

Bastviken, D., Sundgren, I., Natchimuthu, S., Reyier, H., and Gålfalk, M.: Technical Note: Cost-efficient approaches to measure carbon dioxide (CO 2) fluxes and concentrations in terrestrial and aquatic environments using mini loggers, Biogeosciences Discussions, 12, 2357-2380, 2015.

Chanton, J. P., and Whiting, G. J.: Trace gas exchange in freshwater and coastal marine environments: ebullition and transport by plants., in: Biogenic Trace Gases: Measuring Emissions from Soil and Water, edited by: Matson, P. A., and Harriss, R. C., Wiley-Blackwell, Oxford, 98-125, 1995.

Cole, J. J., Bade, D. L., Bastviken, D., Pace, M. L., and Bogert, M. V. d.: Multiple approaches to estimating air-water gas exchange in small lakes Limnology and Oceanography: Methods, 8, 285-293, 10.4319/lom.2010.8.285, 2010.

Deemer, B. R., Harrison, J. A., Li, S., Beaulieu, J. J., DelSontro, T., Barros, N., Bezerra-Neto, J. F., Powers, S. M., dos Santos, M. A., and Vonk, J. A.: Greenhouse Gas Emissions from Reservoir Water Surfaces: A New Global Synthesis, BioScience, 66, 949-964, 10.1093/biosci/biw117, 2016.
DelSontro, T., McGinnis, D. F., Wehrli, B., and Ostrovsky, I.: Size Does Matter: Importance of Large Bubbles and Small-Scale Hot Spots for Methane Transport, Environmental Science & Technology, 49, 1268-1276, 10.1021/es5054286, 2015.
Delwiche, K., and Hemond, H. F.: An enhanced bubble size sensor for long-term ebullition studies, Limnol. Oceanogr. Methods, 15, 821-835, 10.1002/lom3.10201, 2017.
Downing, J. A., Prairie, Y. T., Cole, J. J., Duarte, C. M., Tranvik, L. J., Striegl, R. G., McDowell, W. H., Kortelainen, P., Caraco, N. F., Melack, J. M., and Middelburg, J. J.: The global abundance and size distribution of lakes, ponds, and impoundments Limnology and Oceanography, 51, 2388–2397, 2006.
Duc, N. T., Silverstein, S., Lundmark, L., Reyier, H., Crill, P., and Bastviken, D.: Automated Flux Chamber for Investigating Gas Flux at Water–Air Interfaces, Environmental science & technology, 47, 968-975, 10.1021/es303848x, 2013.
Figaro TGS 2611—for the detection of Methane: http://www.figarosensor.com/products/docs/TGS%202611C00%281013%29.pdf, access: 25.06.15, 2013.
Gålfalk, M., Bastviken, D., Fredriksson, S., and Arneborg, L.: Determination of the piston velocity for water-air interfaces using flux chambers, acoustic Doppler velocimetry, and IR imaging of the water surface, Journal of Geophysical Research: Biogeosciences, 118, 770-782, 10.1002/jgrg.20064, 2013.
Goodrich, J. P., Varner, R. K., Frolking, S., Duncan, B. N., and Crill, P. M.: High-frequency measurements of methane ebullition over a growing season at a temperate peatland site, Geophysical Research Letters, 38, L07404, 2011.
Goulden, M. L., and Crill, P. M.: Automated measurements of CO2 exchange at the moss surface of a black spruce forest, Tree Physiology, 17, 537-542, 10.1093/treephys/17.8-9.537, 1997.
Johnson, M. S., Billett, M. F., Dinsmore, K. J., Wallin, M., Dyson, K. E., and Jassal, R. S.: Direct and continuous measurement of dissolved carbon dioxide in freshwater aquatic systems—method and applications, Ecohydrology, 3, 68-78, 10.1002/eco.95, 2010.
Little, M. A., and Jones, N. S.: Generalized methods and solvers for noise removal from piecewise constant signals. I. Background theory, Proceedings. Mathematical, physical, and engineering sciences / the Royal Society, 467, 3088-3114, 10.1098/rspa.2010.0671, 2011.
Lorke, A., Bodmer, P., Noss, C., Alshboul, Z., Koschorreck, M., Somlai, C., Bastviken, D., Flury, S., McGinnis, D., and Maeck, A.: Technical Note: Drifting vs. anchored flux chambers for measuring greenhouse gas emissions from running waters, Biogeosciences Discuss., 12, 2015.
Luomala, J., and Hakala, I.: Effects of Temperature and Humidity on Radio Signal Strength in Outdoor Wireless Sensor Networks, Acsis-Ann Comput Sci, 5, 1247-1255, 10.15439/2015f241, 2015.
Maeck, A., Hofmann, H., and Lorke, A.: Pumping methane out of aquatic sediments – ebullition forcing mechanisms in an impounded river, Biogeosciences, 11, 2925-2938, 10.5194/bg-11-2925-2014, 2014.
Marotta, H., Pinho, L., Gudasz, C., Bastviken, D., Tranvik, L. J., and Enrich-Prast, A.: Greenhouse gas production in low-latitude lake sediments responds strongly to warming, Nature Clim. Change, 4, 467-470, 10.1038/nclimate2222 http://www.nature.com/nclimate/journal/v4/n6/abs/nclimate2222.html#supplementary-information, 2014.
Meng, L., Hess, P. G. M., Mahowald, N. M., Yavitt, J. B., Riley, W. J., Subin, Z. M., Lawrence, D. M., Swenson, S. C., Jauhiainen, J., and Fuka, D. R.: Sensitivity of wetland methane emissions to model assumptions: application and model testing against site observations, Biogeosciences, 9, 2793 - 2819, 2012.
Ostrovsky, I., McGinnis, D. F., Lapidus, L., and Eckert, W.: Quantifying gas ebullition with echosounder: the role of methane transport by bubbles in a medium-sized lake Limnology and Oceanography: Methods, 6, 105-118, 2008.
Smith, S. V.: Physical, chemical and biological characteristics of CO2 gas flux across the air-water interface, Plant, Cell & Environment, 8, 387-398, 10.1111/1365-3040.ep11660734, 1985.
Tassin, A. L., and Nikitopoulos, D. E.: Non-intrusive measurements of bubble size and velocity, Experiments in Fluids, 19, 121-132, 1995.
Tranvik, L. J., Downing, J. A., Cotner, J. B., Loiselle, S. A., Striegle, R. G., Ballatore, T. J., Dillon, P., Finlay, K., Fortino, K., Knoll, L. B., Kortelainen, P. L., Kutser, T., Larsen, S., Laurion, I., Leech, D. M., McCallister, S. L., McKnight, D. M., Melack, J. M., Overholt, E., Porter, J. A., Prairie, Y., Renwick, W. H., Roland, F., Sherman, B. S., Schindler, D. W., Sobek, S., Tremblay, A., Vanni, M. J., Verschoor, A. M., von Wachenfeldt, E., and Weyhenmeyera, G. A.: Lakes and reservoirs as regulators of carbon cycling and climate, Limnology and Oceanography, 54, 2298-2314, 2009.
Varadharajan, C., Hermosillo, R., and Hemond, H. F.: A low-cost automated trap to measure bubbling gas fluxes, Limnology and Oceanography: Methods, 8, 363-375, 2010.

Verpoorter, C., Kutser, T., Seekell, D. A., and Tranvik, L. J.: A global inventory of lakes based on high-resolution satellite imagery, Geophys. Res. Lett., 41, 6396-6402, 10.1002/2014gl060641, 2014.
Vesala, T., Eugster, W., and Ojala, A.: Eddy covariance measurements over lakes, in: Eddy covariance, Springer, 365-376, 2012.
Walter, B. P., Heimann, M., and Matthews, E.: Modeling modern methane emissions from natural wetlands 1. Model description and results, Journal of Geophysical Research-Atmospheres, 106, 34189-34206, 2001.
Wik, M., Crill, P. M., Varner, R. K., and Bastviken, D.: Multiyear measurements of ebullitive methane flux from three subarctic lakes, J Geophys Res-Biogeo, 118, 1307-1321, 10.1002/jgrg.20103, 2013.
Wik, M., Thornton, B. F., Bastviken, D., Uhlbäck, J., and Crill, P. M.: Biased sampling of methane release from northern lakes: A problem for extrapolation, Geophysical Research Letters, 43, 1256-1262, 10.1002/2015GL066501, 2016a.
Wik, M., Varner, R. K., Anthony, K., MacIntyre, S., and Bastviken, D.: Climate-sensitive northern lakes and ponds are critical components of methane release, Nature Geoscience, 9, 99-105, 10.1038/ngeo2578, 2016b.
Yvon-Durocher, G., Allen, A. P., Bastviken, D., Conrad, R., Gudasz, C., St-Pierre, A., Thanh-Duc, N., and del Giorgio, P. A.: Methane fluxes show consistent temperature dependence across microbial to ecosystem scales, Nature, 507, 488-491, 10.1038/nature13164, 2014.

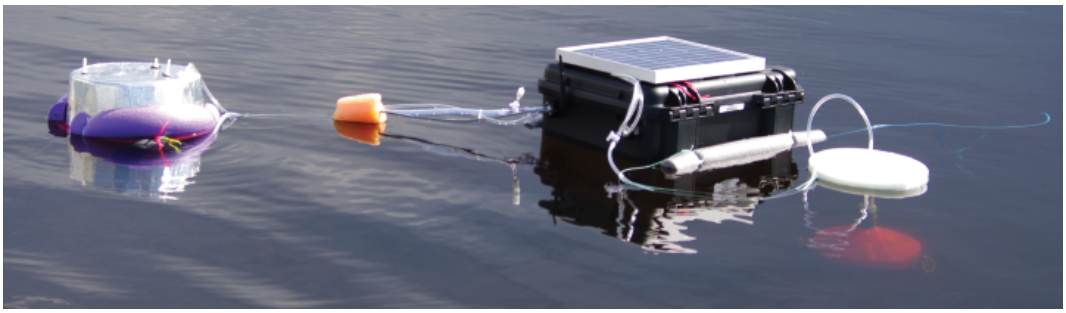

Figure 1: The photo of a deployed AFC_ABC device consists of a floating control box that houses the electronics, a floating chamber and a submerged funnel.

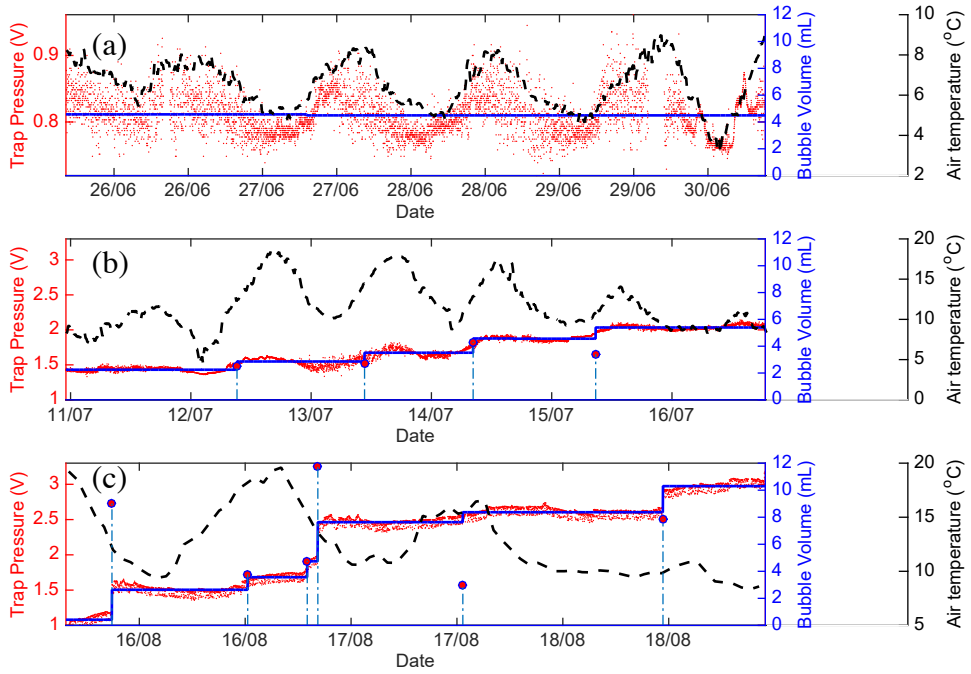

Figure 2: ABC pressure signal and air temperature over three field deployment periods. Red dots are trap pressure signals, blue lines are the denoised pressure sensor signal, stem plots (vertical dashed lines with red circle on top) are bubble events which were detected from the stepwise increase of denoised signals, and black dash are air temperature. (a) Sample period with no bubbles entering the trap, (b) Sample period with small bubbles entering the trap, and (c) sample period with both big and small bubbles entering the trap.

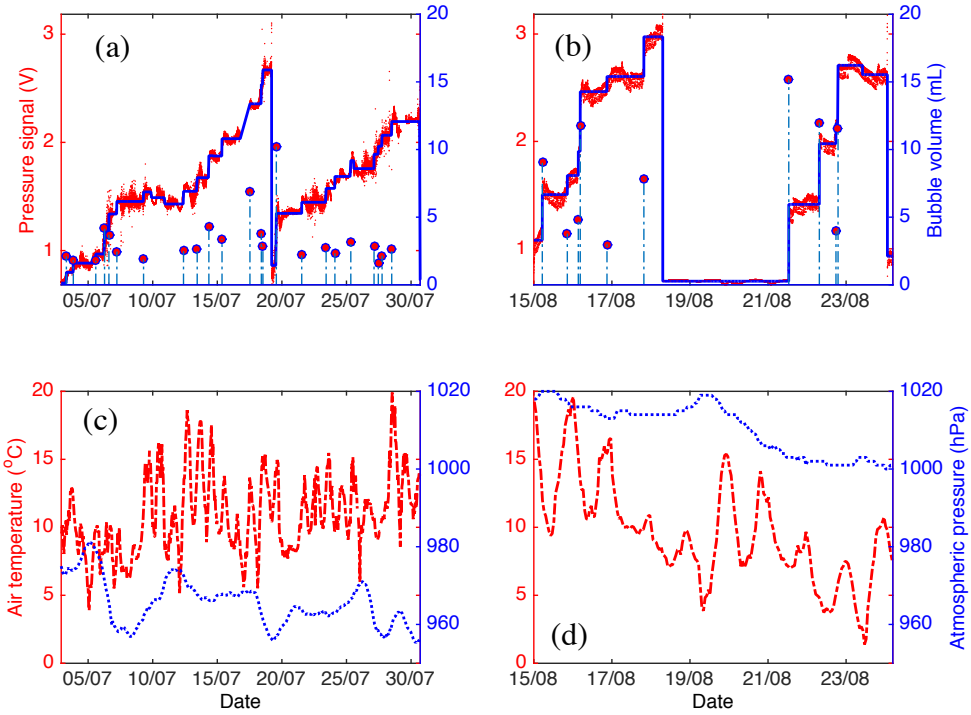

Figure 3: Two measurement periods of an ABC deployed in Mellersta Harrsjön, Stordalen Mire, Abisko in 2015. (a and b) Sample period when bubbles entering the trap were detected from the denoised pressure signal, red dots are trap pressure signals, blue lines are the denoised pressure sensor signal, stem plots (vertical dashed lines with red circle on top) are bubble events. (c and d) Air temperature and atmospheric pressure from an onshore weather station during the same sample period, and red dash are air temperature and blue dots are atmospheric pressure.

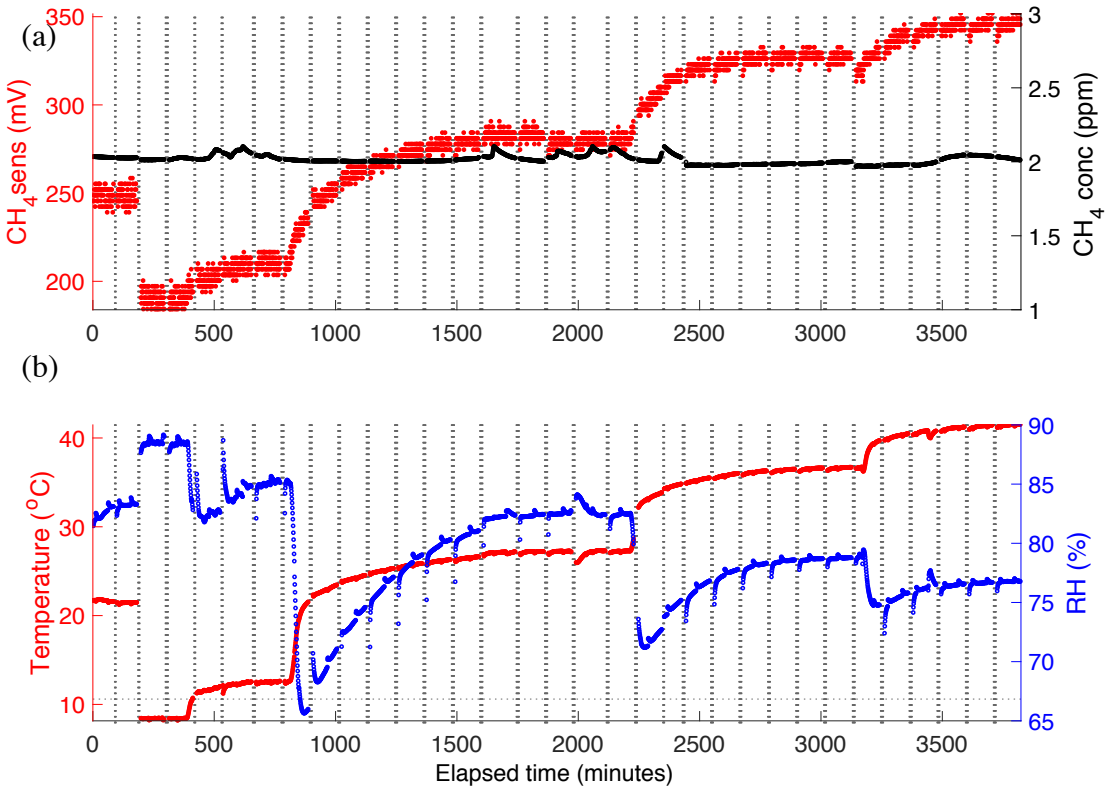

Figure 4: Methane (mV response and concentration), temperature (°C), and RH (%) sensor responses in the initial phase of the sensor test experiment in which temperature of water tank was regulated in range from 5 to 35°C. a) CH_4 sensor signal and actual CH_4 concentration around 2ppm, and b) Temperature and RH in the chamber over the experimental period. Vertical dotted lines denote periods when chamber was opened for ventilation.

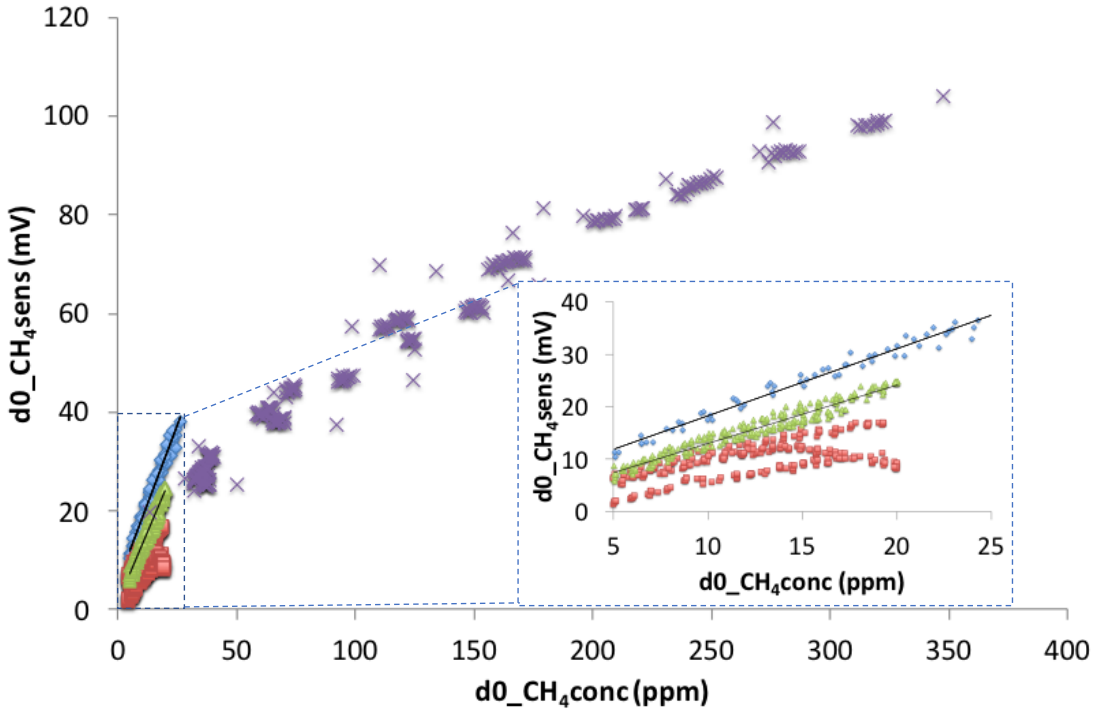

Figure 5: Calibration curves of the CH_4 sensors responses at all experimental water temperatures from 10 to 30°C versus the changing of CH_4 mixing ratio measured by GC-FID or an Los Gatos Research FGGA greenhouse gas analyzer (d0_CH_4conc). The blue diamonds, green triangles and purple crosses (Δ, x: for CH_4 concentration higher than 25 ppm), and red squares represent the change in the CH_4 sensor signal over time from the chamber closure (d0_CH_4sens) of the TGS2611-E00, NGM2611-E13 and the Panterra sensor, respectively. See text for details.

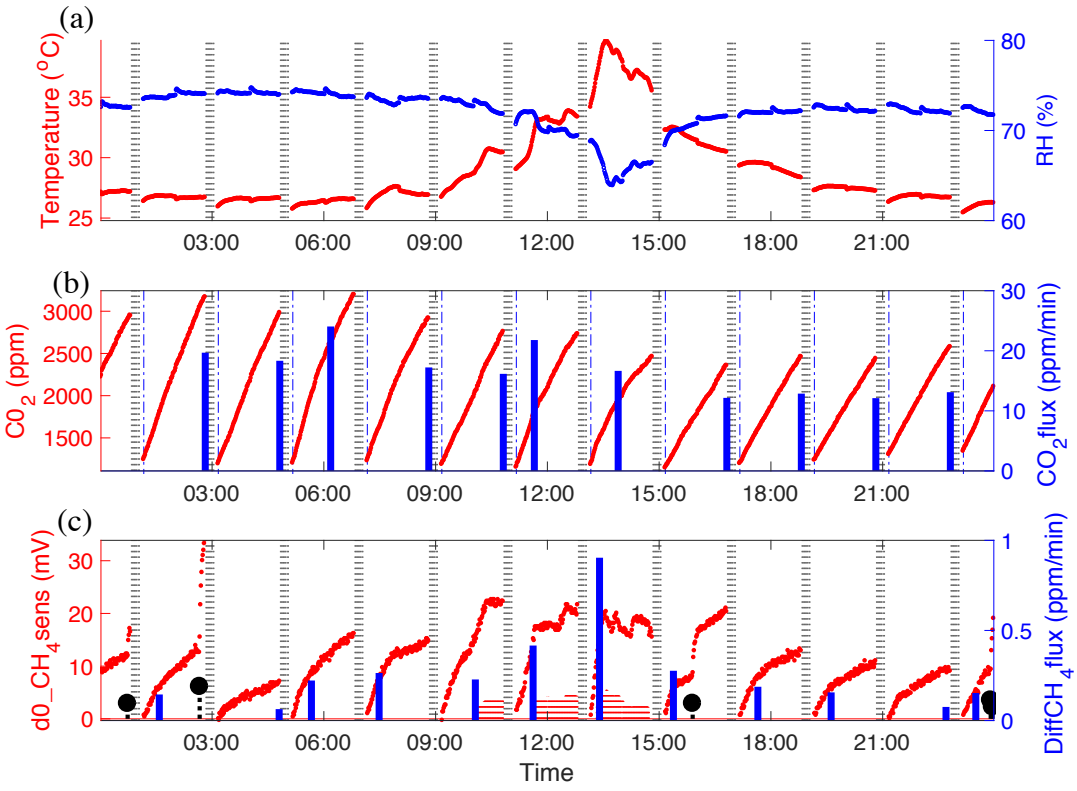

Figure 6: Example of one day of automatic flux chamber (AFC) measurements covering 11 accumulation periods. (a) Scatter plot of temperature (left axis, red) and RH (right axis, blue) in the chamber. (b) Scatter plot of CO_2 concentration measured by an ELG CO_2 sensor (left axis) and bar plot of CO_2 fluxes calculated from slopes of the changing CO_2 concentration in time range marked from the vertical dash dot line to bar plot location (right axis). (c) Scatter plot of CH_4 sensor signal (left axis) and bar plot of CH_4 fluxes (right axis) calculated from the best linear data range when d0_CH_4sens values are in the calibration linear range (less than 30 mV), temperature and RH changes are less than 2°C and 5%. Red shaded periods indicate sampling when temperature and RH are affecting the gas sensor response and therefore these data are not used in the flux calculation. In the event of an ebullition event, the flux calculation is made with data taken prior to that event. Ebullition events are marked by the black stem plot.

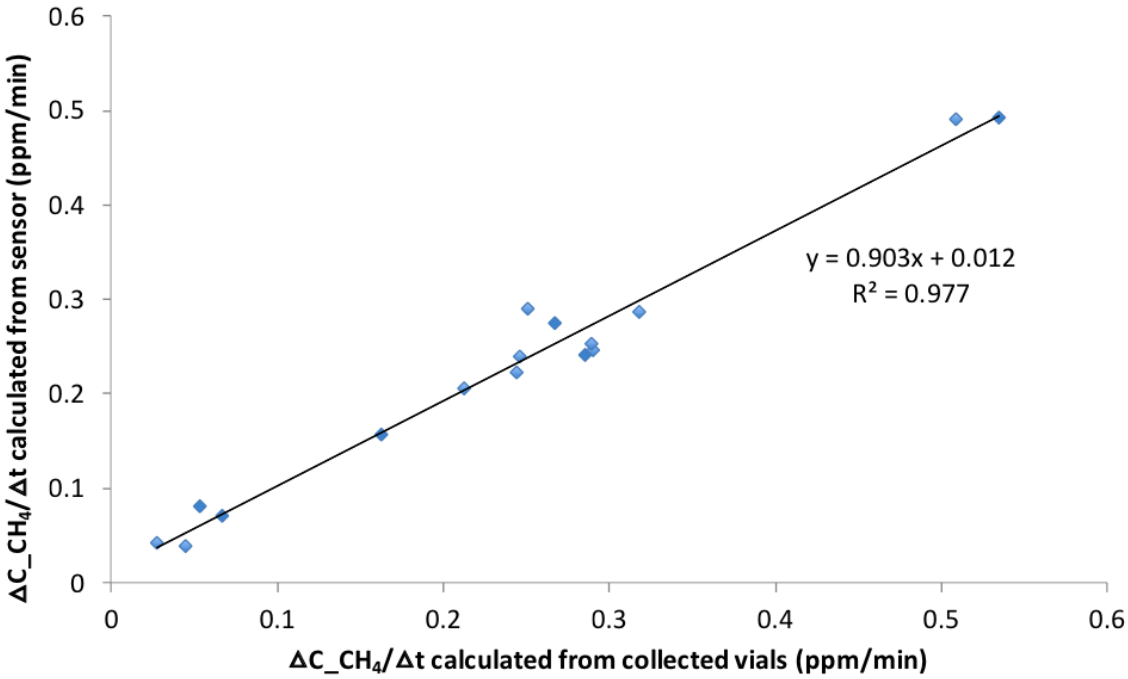

Figure 7: Methane accumulation rates calculated from an NGM2611-E13 CH_4 sensor signal compared to accumulation rates calculated from CH_4 mixing ratio in gas samples collected at the start and end of accumulation periods.